Geologica Acta, Vol.8, Nº 2, June 2010, 169-187
DOI: 10.1344/105.000001528
Available online at www.geologica-acta.com
geologica acta

Modern sedimentation patterns and human impacts on the Barcelona continental shelf (NE Spain)

C. LIQUETE [1] R.G. LUCCHI [1] J. GARCIA-ORELLANA [1] [3] M. CANALS [1] P. MASQUE [2] C. PASQUAL [1] C. LAVOIE [1]

[1] **GRC Geociències Marines, Universitat de Barcelona**
Departament d'Estratigrafia, Paleontologia i Geociències Marines, c/Martí i Franquès s/n, E-08028 Barcelona, Spain.
Liquete E-mail: cliquete@ub.edu ; Lucchi E-mail: rglucchi@ub.edu; Canals E-mail: miquelcanals@ub.edu;
Pascual E-mail: cpascual@ub.edu; Lavoie E-mail: caroline.lavoie@ub.edu

[2] **Institut de Ciència i Tecnologia Ambientals, Universitat Autònoma de Barcelona**
Departament de Física, E-08193 Bellaterra, Spain. Garcia-Orellana E-mail: jordi.garcia@uab.cat;
Masque E-mail: pere.masque@uab.cat

[3] **Marine Sciences Research Center, Stony Brook University**
Stony Brook, New York 11794-5000, USA

ABSTRACT

Seafloor sediments were collected from the Barcelona continental shelf, NE Spain, to determine the textural characteristics and sedimentary processes related to different depositional systems and human pressures. The Barcelona continental shelf is principally influenced by the discharge of the Llobregat and Besòs rivers, and also by anthropogenic modifications such as the diversion of the Llobregat River or the enlargement of the Port of Barcelona.

Sedimentological, physical and biogeochemical properties of 14 sediment cores and grabs indicate the presence of three distinct depositional environments linked to river-influenced, marine-influenced and mixed sedimentation. Sedimentological results have been used to groundtruth available backscatter data. The river-influenced environment, mainly associated to the Llobregat River input, does not reach the shelf edge as the prevailing oceanographic currents deflect sediments south-westward. Riverine sediments are fine-grained, with abundant plant debris, micas and relatively high organic carbon content. The associated sedimentary features are the Holocene prodelta and two modern mud patches. The marine-influenced environment extends north-easterly over the middle and outer shelf and on the upper continental slope. The sediments are coarser grained with abundant bioclasts and lower organic carbon content. Mixed sedimentation is present between the river- and marine-influenced areas. In addition, ^{210}Pb, ^{226}Ra and ^{137}Cs radiometric analyses were used to estimate accumulation rates as well as to identify sites with disturbed sedimentation. Relatively high sediment accumulation rates (up to 0.70-1.03 g·cm^{-2}·yr^{-1} equivalent to 6.4-10 mm·yr^{-1}) are estimated on the Llobregat prodelta while moderate rates (0.21-0.46 g·cm^{-2}·yr^{-1} or 1.6-3.6 mm·yr^{-1}) are found between the Besòs and the Llobregat outlets.

Two sediment cores show a sharp change from river-influenced to marine-dominated conditions that occurred in the mid-1960s. This is interpreted as a significant regression (~2.5 km in 40 years) of the river-influenced domain that may be associated to the extension of the Port of Barcelona and the canalization of the Besòs River, amongst other reasons. Other important human impacts observed in the Barcelona continental shelf are (i) sediment mixing by dredging, ship anchoring and trawling; and (ii) possible organic pollution associated to river and sewage discharges.

KEYWORDS | **Llobregat. Besòs. Prodelta. Continental shelf. Accumulation rate. Human impact.**

INTRODUCTION

Modern continental shelves influenced by densely populated coastal areas and located off river mouths experience complex interactions between continental influences, marine processes and direct and indirect anthropogenic impacts. Studies around the world have demonstrated that changes in fluvial discharge and human activities modify the oceanographic conditions of the shelf waters and the accumulated seafloor sediments (e.g. Dounas et al., 2007; Gao and Ping Wang, 2008; Hartwell, 2008). The Barcelona continental shelf, off the Barcelona city (NE Spain), is a good area to study these complex relationships. The Barcelona area is under the influence of two typical Mediterranean rivers, Llobregat and Besòs, and it is the second European city in population density with more than 4 million people (European Communities, 2000). The disruption of the natural conditions in terms of sediment entry points and dynamics is illustrated by the recent diversion of the Llobregat river mouth and the enlargement of the Port of Barcelona that will occupy nearly one third of the adjacent continental shelf. This extension will likely cause major alterations on oceanographic conditions and sediment-dispersal patterns.

The study of the modern sediment supplies and the sediment distribution on the continental shelf is of great importance to better understand the seafloor morphology, to evaluate ecosystems vulnerability and to anticipate shelf evolution under the pressure of human activities. Previous works based on sedimentological and chemical analyses led, first, to identify the main sedimentary processes shaping the continental shelf off Barcelona and, secondly, to document a record of heavy metal pollution (Palanques and Diaz, 1994; Palanques et al., 1998; Puig et al., 1999; Sanchez-Cabeza et al., 1999; Palanques et al., 2008). Despite these studies, no comprehensive analysis of the fluvial and marine depositional environments in interaction with anthropogenic pressures and their impacts has been completed on the Barcelona continental shelf so far.

In this paper, surface sediment samples and seafloor geophysical data (backscatter) are presented. The aim of the present work is to (i) identify the imprint of the main sedimentary processes resulting from the combination of fluvial and marine influences, and (ii) elucidate the effect of anthropogenic impacts on the shoreline-prodelta-shelf system off the city of Barcelona. To achieve these goals sediment textural, compositional and radiometric data have been integrated with associated backscatter data.

REGIONAL SETTING

The Barcelona continental margin consists of a 6-20 km wide shelf extending down to 110-120 m water depth, and a 25-60 km wide continental slope incised by a series of submarine canyons, such as the Foix Canyon to the south, the Berenguera and Morras troughs on the mid-slope in front of Barcelona, and the Besòs and Arenys canyons to the north (Canals et al., 2004; Amblas et al., 2006) (Fig. 1). In general, the 30 m and 80 m isobaths define the inner-middle and middle-outer shelf boundaries, respectively (ITGE, 1989). The Barcelona continental shelf has a gentle slope (0.6º in average) (Liquete et al., 2007) as well as the continental slope, which is rarely steeper than 4º except for the canyon walls (Amblas et al., 2006).

The Llobregat and Besòs rivers discharge represents the main sediment supply to the Barcelona continental shelf. The Llobregat River, with a watershed of 5045 km^2, flows north-south along 163 km from the Pyrenees to the Mediterranean Sea. The Llobregat Delta, located underneath the city of Barcelona and its suburbs, covers an area of 80 km^2 defined by a coastline of 21 km (Fig. 1). The regime of the Llobregat River is typically Mediterranean with a relatively low mean water discharge and extreme seasonal variations. Mean water discharge between 1967 and 2001 was 16.3 $m^3 \cdot s^{-1}$ at Sant Joan Despí gauging station, at 9.5 km from the river mouth (Fig. 1), where a maximum daily discharge of 1600 $m^3 \cdot s^{-1}$ was measured in November 11th 1982 (Liquete et al., 2009). The Besòs river basin has an area of 1029 km^2 and its main course flows north-south along 52 km from the Catalan Coastal Ranges to the Mediterranean Sea (Fig. 1). The Besòs River forms a delta of 8.3 km^2 with a coastal development of 7.6 km. Mean water discharge between 1968 and 2001 was 6.8 $m^3 \cdot s^{-1}$ at Santa Coloma de Gramenet gauging station, 2.8 km far from the river mouth (Fig. 1), where a maximum daily discharge of 270 $m^3 \cdot s^{-1}$ was measured in May 9th 1991 (Liquete et al., 2009).

The Llobregat and Besòs rivers form coalescent prodeltas that cover 193 km^2 extending NE-SW over the inner and middle shelf. Previous investigations identified a proximal area formed by clean and well sorted sand leading to a seaward belt of muddy sand to mud (Marquès, 1974; Manzano, 1986; ITGE, 1989). The prodelta wedge, with an approximate volume of 2.7 km^3, thins toward the outer shelf where relict sands outcrop in sediment starved areas (Liquete et al., 2008).

On the Barcelona continental shelf, sediment tends to be transported south-westward from the entry points due to the action of (a) the dominant littoral drift, and (b) the Northern Current (NC), a geostrophic current that flows over the continental slope and shows episodic incursions on the continental shelf and some semi-

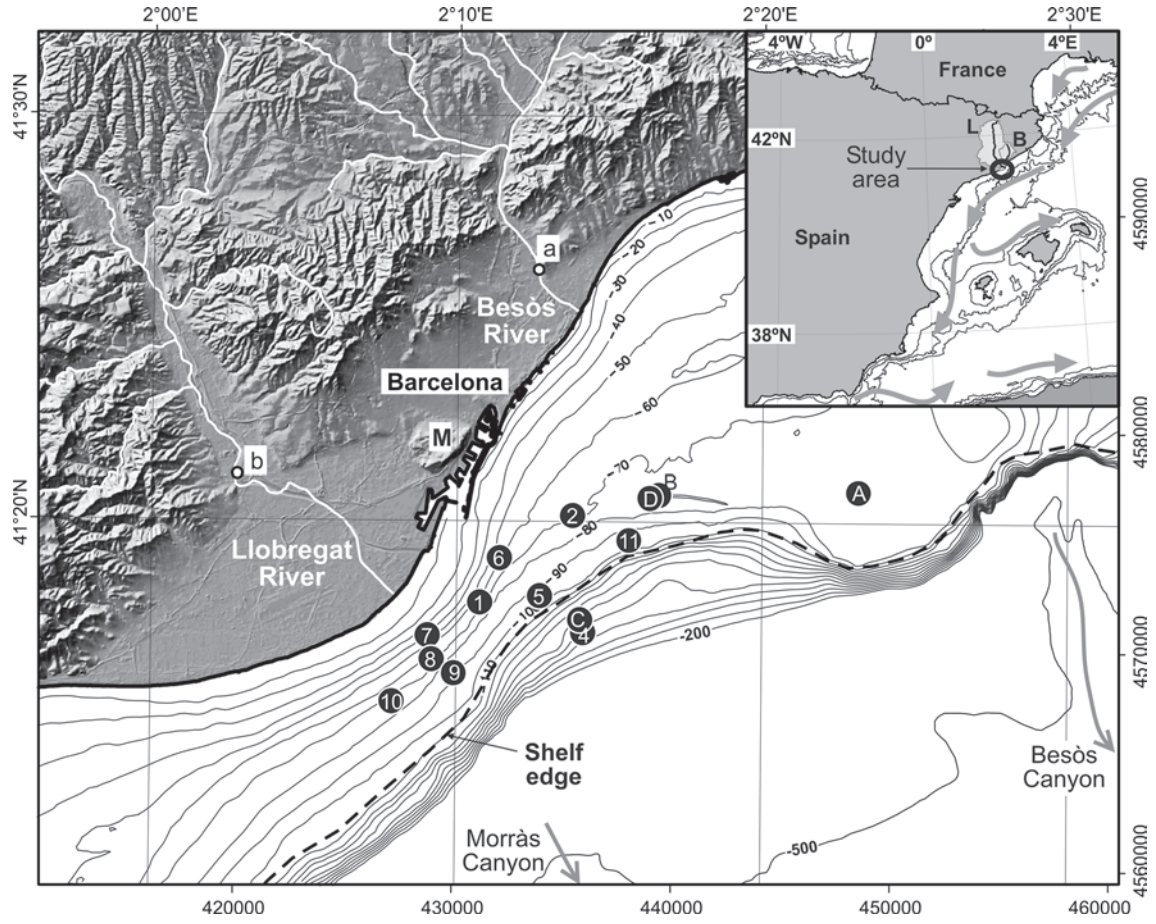

FIGURE 1 | **Topographic map of the study area showing the location of the surface sediment samples. Letters "a" and "b" point to the gauging stations mentioned in the text, "Santa Coloma de Gramenet" and "Sant Joan Despí", respectively. "M" points to the Montjuic hill. Arrows in the top-right diagram indicate the main surface oceanographic currents after Millot (1999).**

permanent mesoscale features (Font et al., 1995; Flexas et al., 2002; Rubio et al., 2005). Castellón et al. (1990) measured spring peak velocities of the NC of 25-30 $cm \cdot s^{-1}$ in the surface waters over the upper slope offshore Barcelona. Fine-grained suspended sediments derived from river's plumes or storm's sediment resuspension can be transferred to the slope and beyond through four permanent nepheloid layers (Puig and Palanques, 1998). Nepheloid layers originated on the Barcelona shelf may be trapped into the Foix submarine canyon head from where particles, and eventually pollutants, are transferred to deeper environments (Sanchez-Cabeza et al., 1999; Palanques et al., 2008).

MATERIAL AND METHODS

This study integrates information from 14 surface sediment samples and a high-resolution multibeam bathymetry survey with associated backscatter data.

Surface sediment samples

Sediment samples were obtained during the oceanographic cruise PRODELTA (September 2004) on board of the R/V García del Cid. Surface sediment samples up to 36 cm long were collected using a multi-corer device (10 sites) and, where the multi-corer could not penetrate due to coarse-grained seafloor sediments, a box corer was used (4 sites) (Table 1 and Fig. 1). The multi-corer recovered 3 cores from each site. Two of them were systematically sampled for laboratory analyses every 0.5 cm in the upper 5 cm, every 1 cm down to 20 cm core length, and every 2 cm until the core bottom. The third core was visually described and tested with a Geotester Pocket Penetrometer to determine the unconfined compressive strength.

All the wet sediment samples were weighted and dried at 50°C in the laboratory. Dry samples were weighted to calculate dry density, water content and porosity. Selected sediment samples were then sub-sampled for grain size,

TABLE 1 | **Location and number of analytical measures of the surface sediment cores and samples.**

	Location				Number of analytical measures						
Sediment core	Total length (cm)	Water depth (m)	Lat. N	Long. E	Pocket penetr.	Water content	Grain size	Micros.	Organic matter	Alpha spectr.	Gamma spectr.
L-1	24	64.6	41.300	2.182	0	27	11	4	1	13	5
L-2	24	69.0	41.337	2.231	9	27	11	4	1	26	12
L-4	17	149.5	41.289	2.237	0	22	9	6	1	20	12
L-5	24	95.8	41.304	2.214	0	27	9	4	1	19	6
L-6	36	57.0	41.320	2.192	9	33	11	4	1	17	8
L-7	36	40.0	41.287	2.153	0	33	11	4	1	14	3
L-8	34	66.3	41.277	2.155	10	32	11	4	1	25	6
L-9	24	84.5	41.272	2.167	9	27	11	4	1	15	5
L-10	23	71.0	41.260	2.133	8	27	11	4	1	18	4
L-11	8	92.0	41.327	2.262	4	13	7	4	1	13	5
L-A	~ 5	72.0	41.347	2.387	0	1	2	1	1	0	0
L-B	~ 5	70.8	41.346	2.279	0	1	2	1	1	0	0
L-C	~ 5	132.0	41.294	2.236	0	1	2	1	1	0	0
L-D	~ 5	69.5	41.345	2.274	0	1	2	1	1	0	0

optical microscope, biogeochemical and radiometric analyses (Table 1).

Sedimentology

For grain size analyses, 96 samples of ~0.8 g of dry sediment were first treated to remove organic matter by two consecutive 24-hours attacks of H_2O_2 at 10%. Next, the samples were treated with HCl at 3% during 3 hours to remove carbonated components. A second set of 14 samples between 0.5-1 cm below seafloor were analyzed without HCl treatment in order to check grain size variations related to the presence of carbonate particles and make a semi-quantative interpretation of the backscatter mosaic.

A Coulter Counter LS100 was used to determine the grain size distribution of the fraction finer than 1 mm. A solution of sodium polyphosphate at 5% was mixed with sediments and smoothly shivered during a few hours before the analyses to complete the grains deflocculation. For the samples containing a sediment fraction >1 mm, the grain size was recalculated on the basis of the dry weight of such fraction. Grain size fractions were classified according to the Udden-Wentworth scale (after Pettijohn et al., 1987) whereas textural statistical parameters were calculated arithmetically by the Coulter Counter software using the following formulae:

Mean size: $\bar{u} = \sum u_i \times n_i / \sum n_i$
Standard deviation: $SD = \sqrt{[\sum (n_i (u_i - \bar{u})^2) / \sum n_i]}$
Skewness: $S = \sum (n_i (u_i - \bar{u})^3) / (SD^3 \sum n_i)$

Where u_i is the center size of the "i" Coulter Counter channel, and n_i is the percentage of particles in the "i" channel. We will use these simple statistical parameters as standard deviation (sorting) and skewness to better describe the depositional environment and the sedimentary processes that have generated the deposit (e.g. Friedman, 1967; Visher, 1969; McLaren and Boweles, 1985; Sutherland and Lee, 1994).

Moreover, qualitative sediment composition was determined through optical microscope investigation on the sand fraction after wet sieving at 63 μm.

Biogeochemical analyses

Total carbon (TC), total nitrogen (TN) and organic carbon (OC) contents were determined from the top 0.5 cm of 12 sampled sites using a Thermo NA 2100 Elemental Analyzer. Uncertainties were lower than 0.1% as determined from replicates of the Canadian National Research Council certified estuarine sediment MESS-1. TC and TN were measured from HCl-untreated samples. The samples for OC determination were attacked successively with HCl at 25% until no effervescence was observed and dried at 60ºC following the methodology described by Nieuwenhuize et al. (1994). Carbonate content (assuming all inorganic carbon is calcium carbonate, $CaCO_3$=(TC-OC)×8.33) and C/N atomic ratio (OC/TN) were calculated. C/N ratios are usually employed to determine the provenance of buried organic matter. In general, algal organic matter shows C/N ratios ranging between 5 and 10 (Emerson and Hedges, 1988; Stein, 1991; Meyers, 1994), while vascular plants have N-free biomolecules that lead to C/N ratios larger than 15 (Stein, 1991) or 20 (Emerson and Hedges, 1988; Meyers, 1994; Hedges et al., 1997).

Radiometric analyses

^{210}Pb activity in multi-corer sediments was determined through the measurement of its grand daughter nuclide

^{210}Po in equilibrium, following the methodology described by Sanchez-Cabeza et al. (1998). Aliquots of 100-200 mg were totally digested by using an analytical microwave oven after addition of ^{209}Po as internal tracer. Plated onto high purity silver discs, polonium isotopes were counted by alpha spectrometry with low background PIPs detectors (CANBERRA). ^{226}Ra and ^{137}Cs were determined by gamma spectrometry using calibrated geometries on an n-type coaxial HPGe ORTEC detector. Uncertainties were calculated by standard propagation of the 1 sigma counting errors of samples and blanks.

Excess ^{210}Pb ($^{210}Pb_{xs}$) was determined by subtracting the activity of the constant ^{210}Pb activities in the deep sections of the sediment cores ($^{210}Pb_{supported}$) from the total ^{210}Pb activity. Since cores L-6, L-7, L-8 and L-11 were too short to determine $^{210}Pb_{supported}$ values, $^{210}Pb_{xs}$ was estimated in these cores by the difference of total ^{210}Pb and ^{226}Ra. Apparent accumulation rates were calculated based on the $^{210}Pb_{xs}$ decay in the unperturbed sections of the cores using the CF:CS model (Goldberg, 1963). Mass accumulation rates were calculated by linear regression of the log for $^{210}Pb_{xs}$ activity data *versus* cumulative mass ($g \cdot cm^{-2}$) using measured dry-bulk densities. Apparent sediment accumulation rates obtained from ^{210}Pb CF:CS models are maximum because the compaction effect and the possible slight along-core mixing caused by human, physical or biological activities are not considered.

The accumulation rates and age models were constrained by ^{137}Cs data considering the onset of the concentration profile as marker of the beginning of the atmospheric testing of nuclear weapons (1954), the deepest subsurface maximum related to the maximum of global fallout (1963), and the shallowest peak corresponding to the Chernobyl accident (1986).

Backscatter data

Backscatter data were acquired with a multibeam echosounder Simrad EM-3000D onboard the 12 m long Arraix boat between March and August 2004. Total coverage attains 625 km^2. Technical details can be found in Liquete et al. (2007). The unprocessed backscatter mosaic represents the amount of acoustic energy that is scattered back from the seafloor. The recorded backscatter data were equalized to highlight the contrasts in digital number values (DN from 0 to 255) to allow semi-quantitative comparisons with the sedimentological results. The amount of backscattered energy may be influenced by the surface roughness, impedance contrast, volumetric heterogeneity, particulate sulfur concentration and/or benthic communities (Blondel and Murton, 1996; Borgeld et al., 1999; Urgeles et al., 2002; Nitsche et al., 2004; Sutherland et al., 2007), but amongst all these factors the backscatter strength is typically linked to sediment grain size (e.g. Blondel and Murton, 1996; Goff et al., 2000; Urgeles et al., 2002; Edwards et al., 2003; Collier and Brown, 2005; Sutherland et al., 2007). Generally, coarser grains are related to high backscatter intensity.

RESULTS AND INTERPRETATION

Sedimentological and biogeochemical properties

Grain-sized analyses, microscope qualitative determination and biogeochemical properties indicate the presence of three distinct depositional environments on the Barcelona continental shelf: river-influenced, marine-influenced and mixed environments.

In general, in all cores the upper sediments are coarser-grained. In most of the cores the sand fraction is dominated by the very-fine (63-125 μm) and fine-grained (125-250 μm) sub-fractions (Fig. 2 and Appendix). Water content and porosity trends are rather similar in all samples showing progressive down-core decreases (Fig. 2). Some punctual variations of this trend usually correspond to grain size changes. As expected, the unconfined compressive strength presents an opposite trend, with higher values at the core base where sediments are more compacted (Fig. 2). Usually, the unconfined compressive strength increases considerably from 5-10 cm depth to the core base, although in core L-11 this increase occurs at only 3 cm depth. Organic matter C/N ratio shows transitional values between algae and vascular plants, from 16 to 8, with a general seaward decreasing trend.

River-influenced environment

Cores L-1, L-6, L-7, L-8, L-9, L-10 and the lower part of core L-4 (from 5 cm depth to the core bottom) present major river inputs. Based on the grain size triangle subdivision of Shepard (1954) (Fig. 3A), cores L-1, L-6, and L-7 contain predominantly sandy silt sediments with mean grain sizes ranging between 10 and 26 μm (fine-medium silt). Cores L-8, L-9, L-10 and the lower part of core L-4 contain clayey silt sediments with mean grain sizes between 10 and 14 μm (fine silt). In general, grain size is larger in the HCl-untreated surface samples than in the respective HCl-treated ones (Fig. 3B) indicating that carbonate grains, usually bioclasts, are relatively large. The only exceptions are L-8, L-9 and L-10 samples where the sparse carbonate fraction seems to be represented by fine-grained calcite. Generally, all grains are badly sorted and slightly negatively skewed (i.e. with high percentage of silt and clay trapped within coarser grains), reflecting probable fluvial conditions (see Appendix). Predominant terrigenous components formed by abundant micas, quartz, dark minerals, Fe-oxides, rock

fragments and rarely calcite were identified by microscope analyses. A minor fraction of bioclasts comprises benthic foraminifera and echinoid spines. These sediments contain also abundant plant debris and display relatively high values of organic carbon (between 0.99 and 1.65%), relatively low carbonate contents (between 20 and 30%), and relatively high C/N ratios (between 12 and 16) (Table 2 and Fig. 4). In general, river influence on sediment properties progressively diminishes seaward and south-westward as grain size increases.

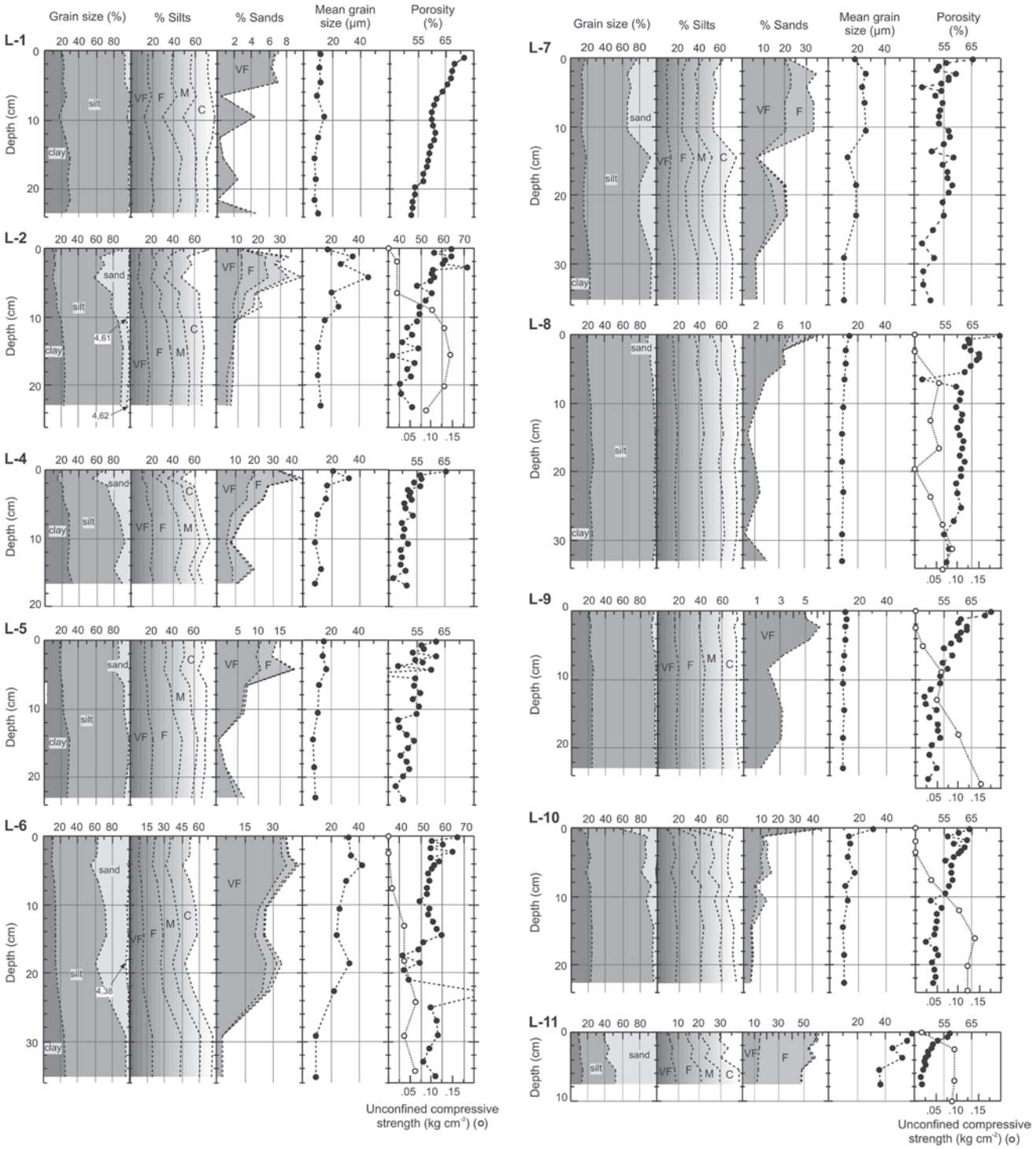

FIGURE 2 | **Down-core logs of grain size and physical properties of the studied sediment cores. VF= very fine; F= fine; M= medium; C= coarse. See location in Fig. 1.**

Marine-influenced environment

The composition of sediments from sites L-A, L-B, L-C, L-11 and the upper part of core L-4 shows a clear marine influence. Sediments in L-A, L-B and L-C contain abundant sand, gravel and carbonates. The siliciclastic component of these samples (HCl-treated material) ranges between fine silt (L-B ~12 μm) and fine sand (L-A ~160 μm), while the bulk sediments with carbonates (HCl-untreated material) range between very fine sand (L-B ~83 μm) and fine sand (L-A ~229 μm) (Fig. 3B). L-11 samples are entirely composed of silty sand (Fig. 3A) with mean grain size of 47 μm (coarse silt). The upper 5 cm of core L-4 show a mean grain size of 21 μm (medium silt). In general, the bulk sediments of all these samples are typically unsorted due to the large variety of bioclasts, while the siliciclastic component is negatively skewed and better sorted than the river-derived material (see Appendix). Marine-derived sediments are characterized by typical shelf fauna with predominant bioclasts of bryozoa, bivalves, gasteropods, ostracods, echinoid spines, sponge spicules, pteropods and benthic and planktonic foraminifera. Abundant micrite is present in the form of faecal pellets. A minor terrigenous fraction is formed by micas and quartz, with rare calcite. In core L-11, the terrigenous fraction is more abundant and very well sorted, with rounded quartz minerals having high sphericity. The OC content within the marine-derived sediments ranges from 0.29 to 0.50% (the lowest values of the study area), while carbonates represent 33-54% (the largest values obtained), and C/N ratios range between 8 and 12 (the lowest values measured) (Table 2 and Fig. 4).

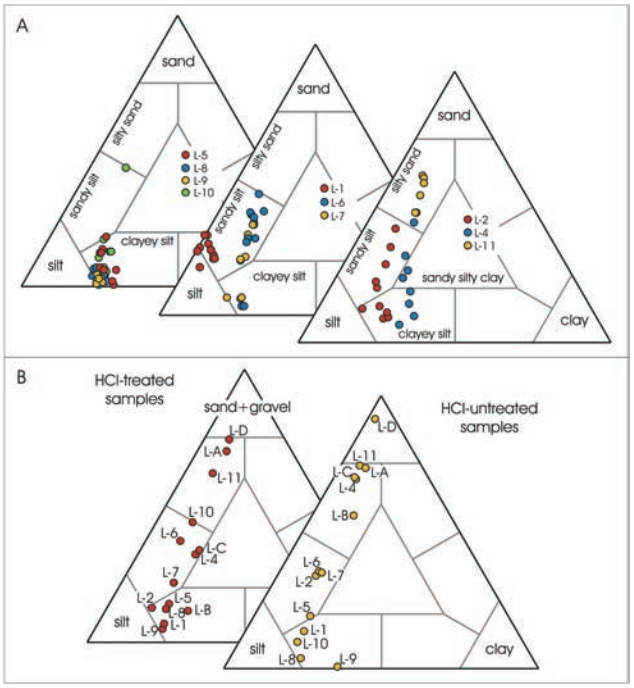

FIGURE 3 | **A) Grain size data of the entire sediment cores used in this study following the sediment classification for unconsolidated sediments of Shepard (1954). Cores are grouped according to their sedimentary similarity. B) Grain size distribution of the surface samples comparing HCl-treated and untreated samples.**

Abundant authigenic glauconite is observed as infilling of foraminifer shells. Glauconite is an aluminosilicate that forms by dissolution of the host mineral, precipitation in micropores and later maturation (Odin and Matter, 1981). The glauconitic minerals found in modern continental shelves may come from recent formation or from erosion of ancient deposits (e.g. Amorosi, 1995). In the modern oceans, these minerals form between 50 and 500 m depth, at sites of slow sediment accumulation and in reducing and confined environments (Logvinenko, 1982; Odin, 1988; Bremner and Willis, 1993; Rao et al., 1993).

TABLE 2 | **Biogeochemical results of the surface sediment samples.**

Surface sediment sample	% OC	% TC	% CaCO3	C / N
L-1	1.65	4.07	20.19	16
L-2	0.70	3.52	23.49	14
L-4	0.48	4.92	36.99	12
L-5	0.80	4.33	29.40	13
L-6	1.02	3.86	23.66	13
L-7	1.07	4.60	29.40	15
L-8	1.62	5.00	28.16	15
L-9	0.99	4.51	29.32	12
L-10	1.22	4.47	27.07	15
L-11	0.31	4.81	37.50	10
L-A	0.30	6.74	53.62	8
L-B	0.29	4.30	33.40	10

Mixed environment

Admixture of bioclastic and terrigenous components are observed in cores L-2, L-5 and L-D. The upper part of core L-2 shows a remarkable decrease of fine mineral components (Fig. 2) and an increase of large bioclasts and biogenic fragments. L-2 contains sandy silt in the upper 9 cm with mean grain size of ~29 μm (medium silt) and clayey silt down-core (~13 μm, fine silt) (Fig. 3A). L-5 is characterized by clayey silt sediments with mean grain size of 12 μm (fine silt). The siliciclastic component of L-D is fine sand (~148 μm) while the bulk sediment is medium sand (~455 μm). Cores L-2 and L-5 contain predominantly marine bioclastic material, although the textural characteristics (near symmetrically skewed sediments), the abundant mica, the presence of plant debris, and the moderate OC content (0.7-0.8%) and C/N ratio (13-14) (Table 2, Fig. 4 and Appendix) indicate a

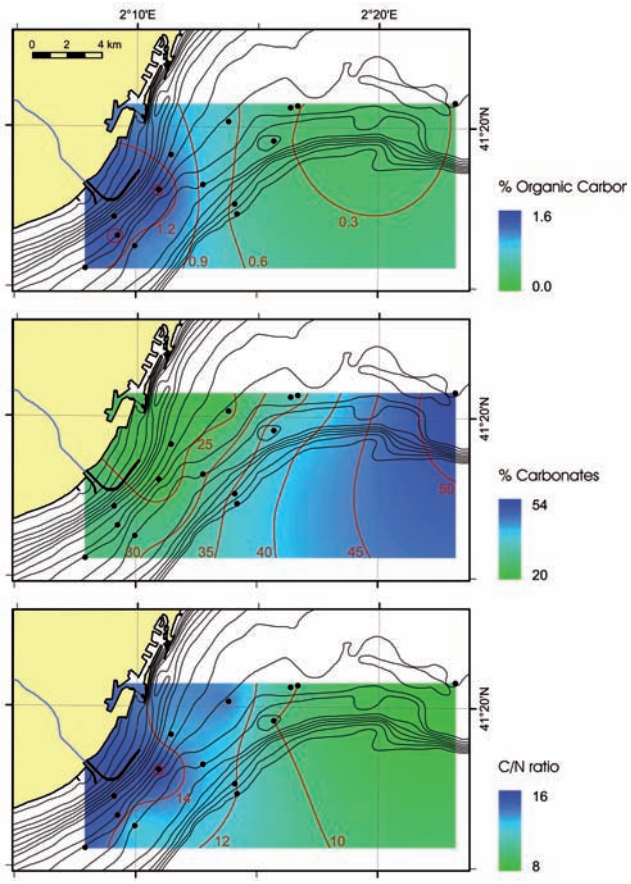

FIGURE 4 | **Gridded distribution of organic carbon, calcium carbonate and C/N ratio in surface sediments. Gridding method is kriging with a spherical variogram. Black dots correspond to the surface sediment samples located in Fig. 1. Black thin lines represent bathymetric contours every 10 m and bold lines are isolines of the represented parameter.**

relevant fluvial influence. Sites L-2 and L-5 are interpreted as the border between the river- and the marine-influenced domains. Sediment sample L-D contains abundant sand and bioclasts and a large variety of rock fragments including granitoids, metamorphic and clastic rocks. The mixed composition of this sample and direct observations during the PRODELTA survey suggest that L-D probably contains dumped sediments from the submarine works of the Port of Barcelona.

Backscatter mosaics and surface sediments

Sea bed textural maps from ITGE (1989) following Shephard's classification (1954) and backscatter data from Liquete et al. (2007) have been integrated with the sedimentological and biogeochemical results from this study (Fig. 5). Most of our HCl-untreated surface samples show a grain size slightly coarser than the corresponding data from ITGE (1989), some of them are identical (L-8, L-9, L-10 and L-D) and only two are slightly finer (L-A and L-B).

The backscatter mosaics from the study area provide continuous data that allow developing an accurate semi-quantitative seafloor characterization. The Barcelona continental shelf backscatter values have been classified into 5 strength DN classes that correlate reasonably well with the grain size classification of ITGE (1989) (Fig. 5). The very low and low backscatter classes roughly correspond to clayey silt; the medium backscatter is produced by sandy silty clay; and the high and very high backscatter is due to the presence of sand and silty sand sediments. Figure 6 shows (i) a significant linear correlation between the backscatter DN and the grain size of the HCl-untreated surface samples, and (ii) the existence of two groups, one with DN between 90 and 140 and another with DN between 160 and 200. The first group is essentially associated with river-influenced sediments found on the prodelta area, while the second group corresponds to coarser marine-influenced sediments located outside the prodelta limit.

Backscatter data show also two very low intensity patches linked to the Besòs and Llobregat outlets extending 6.5 and 13 km south-westward, respectively. These patches are tentatively linked to particles settling from hypopycnal river plumes (Liquete et al., 2007). Cores L-8, L-9 and L-10, recovered at the limit of one of these patches, show relatively homogeneous very fine (clayey silt) river-influenced material. The highest backscatter intensities, generally constrained to the middle and outer shelf to the north of the Llobregat River, are interpreted as coarse material (probably relict sands) barely covered by fine-grained modern sediments. The highest backscatter data reflect the presence of several bedforms like the sediment waves of the Llobregat prodelta front ("a" in Fig. 5), the sand bars discernible in the outer shelf to the north of Barcelona ("b" in Fig. 5), or the seafloor impacts caused by the enlargement works of the Port of Barcelona ("c" in Fig. 5) (Liquete et al., 2007; Urgeles et al., 2007).

The minor differences between ITGE (1989) textural maps and the new backscatter mosaics can be attributed to i) changes in surface sediment distribution between 1986-88 and 2004, when the corresponding surveys were carried out, ii) local influence of factors other than surface roughness in the backscatter intensity, or iii) inaccuracies due to the lower resolution and gridding method of the ITGE data, and also to poor positioning accuracy as ITGE surveys were done in pre-DGPS times. Although we cannot ignore any of these possibilities, the last one is considered the most important.

Radiometric analyses

Total ^{210}Pb activity profiles present evident signals of sediment mixing in several cores (Fig. 7). The river-

influenced L-1, L-9 and L-10 cores show a similar pattern with an upper mixing layer of 2.5, 7.5 and 7.5 cm, respectively, and a constant profile below section 7.5, 8.5 and 9.5 cm, respectively. In these three cores, mean ^{210}Pb value of the basal sections is still higher than the concentrations of ^{226}Ra and, for example in the L-1 case, the assumption of an unperturbed base level of ^{210}Pb below 7.5 cm would be incompatible with the presence of ^{137}Cs

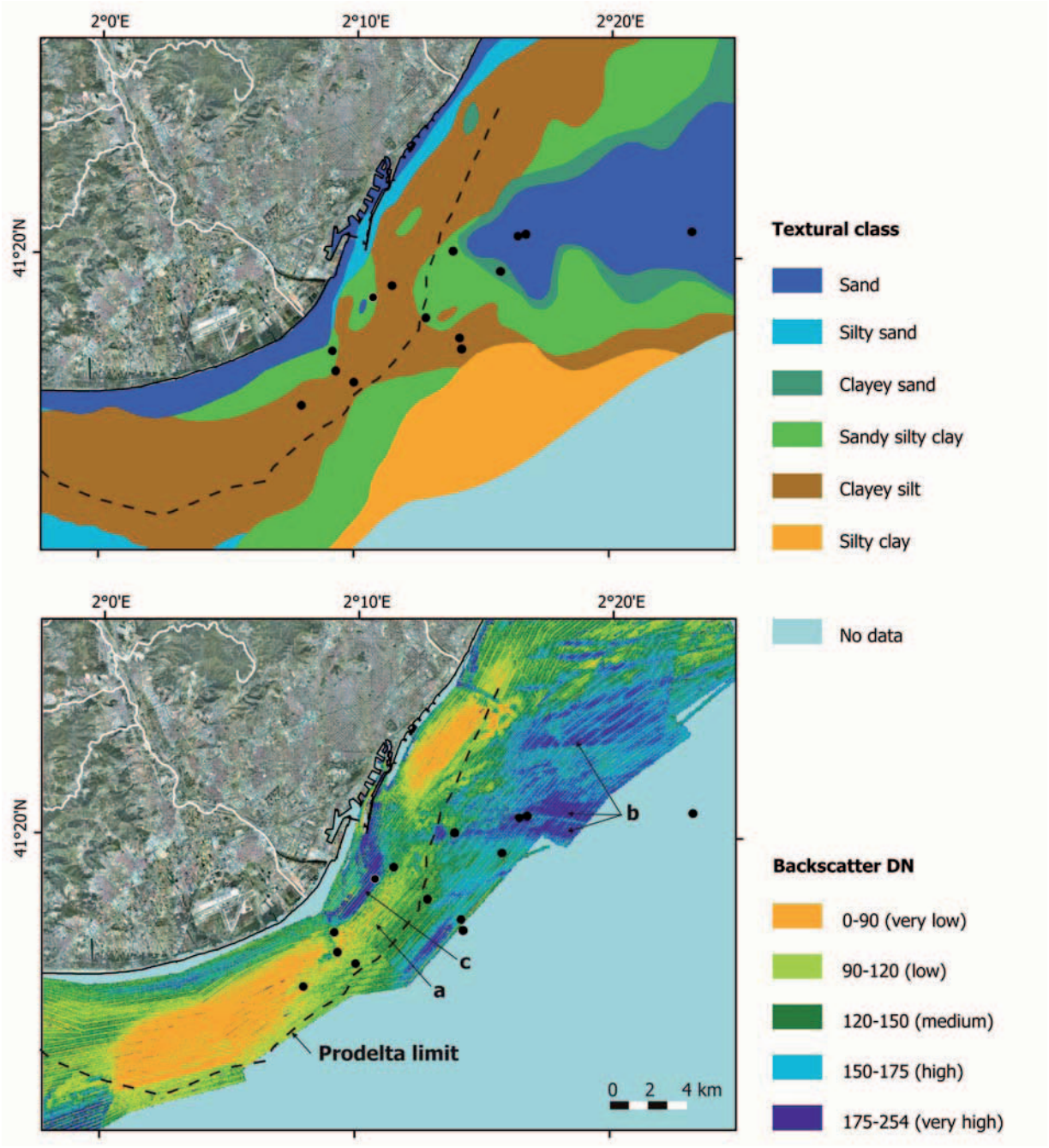

FIGURE 5 | **Sea bed textural map from ITGE (1989) (upper map) and backscatter mosaic from the Barcelona continental shelf (bottom map). Black dots correspond to the surface sediment samples analyzed in this study. The dashed line points to the outer prodelta limit as defined by Liquete et al. (2008). DN: digital number indicating the backscatter magnitude. a) sediment waves on the Llobregat prodelta front; b) sand bars on the outer shelf; c) seafloor impacts caused by the enlargement works of the Port of Barcelona. The ortophotomap onland shows the densely populated and industrialized coastal area and the old Llobregat river mouth deviated in 2004. Map projection is UTM zone 31N datum WGS84.**

at 19.5 cm. Even if we considered that the ^{210}Pb at the core bottom is the $^{210}Pb_{supported}$, the resultant concentrations of $^{210}Pb_{xs}$ could be calculated from only two measurements in core L-9 and three measurements in cores L-1 and L-10, which is insufficient to infer accumulation rates. Therefore, L-1, L-9 and L-10 are considered too short for a ^{210}Pb chronology reconstruction and practically whole mixed, according to the ^{210}Pb activity profiles and the relatively constant grain size and sedimentological composition. This is the most plausible interpretation since the sampling sites are within the trawling zone and close to the anchor and dredging areas of the Port of Barcelona. However, and alternative explanation could be that these cores show very high and variable sedimentation rates, as typical from prodeltaic areas.

River-influenced cores L-6, L-7 and L-8 present continuous and slightly decreasing activity profiles with small deviations (Fig. 7), which could be linked to sediment mixing or very high accumulation rates. Radiometric results point to sediment mixing in the top 12.5 cm of L-7. L-6, L-7 and L-8 seem too short to reach the base of the ^{210}Pb activity profile ($^{210}Pb_{supported}$) and, hence, ^{226}Ra is used instead of ^{210}Pb at the bottom core to estimate $^{210}Pb_{xs}$ and the derived accumulation rate (Table 3). The same procedure was applied to core L-11, which shows an upper mixed layer of 3.5 cm. The detection of ^{137}Cs in the bottom part of these cores supports this approach and restricts the possible chronology to the second half of the 20th century. Maximum apparent accumulation rates can be estimated for these cores, but it should be taken into account that they could present slight sediment mixing along them.

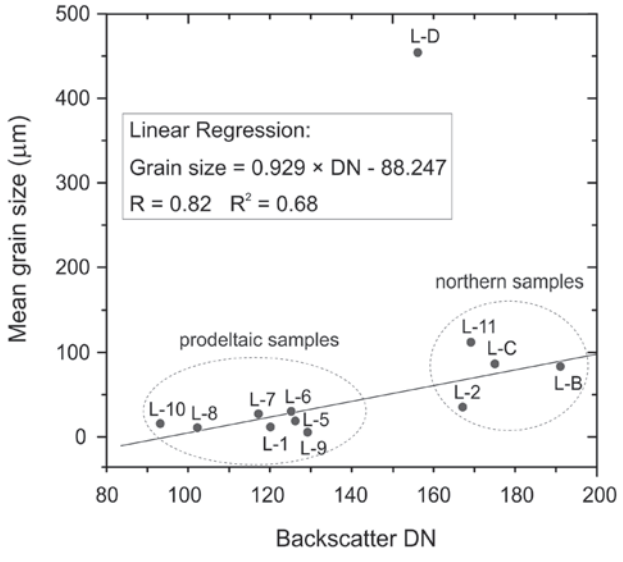

FIGURE 6 | **Bivariate plot of backscatter digital number (DN) *versus* surface sediment mean grain size of HCl-untreated samples. The linear regression ignores surface sample L-D as an outlier. Samples L-A and L-4 are not represented because they lie beyond the backscatter data coverage (see Fig. 5).**

The total ^{210}Pb activities from cores L-2, L-4 and L-5 show an exponential decay profile that indicates a continuous sedimentation (Fig. 7). $^{210}Pb_{supported}$ and ^{226}Ra activities are in general coincident, ranging between 23±3 and 29±4 Bq·kg^{-1} (Table 3). Still, while core L-2 shows an undisturbed ^{210}Pb profile, cores L-4 and L-5 present signs of mixing in their upper 2.5 and 7.5 cm, respectively (Fig. 7). Both ^{210}Pb and ^{137}Cs nuclides give a congruent geochronology.

Radiometric analyses of L-4 and L-11 sediments, where glauconite was observed, indicate that they were deposited during the last 100-150 years. These measures would agree with previous studies (e.g. Nelsen et al., 1994; Fernández-Bastero et al., 2001) that propose a decadal time scale for glauconite formation instead of the traditional thousand-to-million years rate (e.g. Odin and Matter, 1981; Odin, 1988). However, some glauconitic grains show a relatively mature aspect reflected by dark green colour, coarser size, and advanced dissolution of the host mineral. The terrigenous component of L-11 is very well sorted and very negatively skewed (see Appendix) with highly spherical and rounded quartz grains. This textural facies is consistent with that of sand beaches in which the persistent mechanical action of the waves on sediments generate grain's abrasion and depletion of the fine fraction. In addition, L-11 presents relatively low ^{210}Pb and ^{137}Cs concentrations. Therefore, we suggest that some of the sediment contained in L-11, and possibly also in L-4, in particular the coarsest fraction, is likely reworked from ancient shelf deposits like relict sand beaches.

Accumulation rates on the Barcelona continental shelf

The radiometric results of cores L-2, L-4, L-5, L-6, L-7, L-8 and L-11 allow estimating maximum apparent sediment accumulation rates at different locations of the Barcelona continental shelf (Fig. 8 and Table 3). Mass accumulation rates range from 0.21 to 1.03 g·cm^{-2}·yr^{-1} (1.6-10.0 mm·yr^{-1}) (Table 3). Maximum rates are found off the Llobregat River (L-6, L-7 and L-8) while minimum values are measured in the outer shelf (L-5) or upper slope (L-4) between the Besòs and the Llobregat river mouths.

The apparent sediment accumulation rates measured on the Barcelona continental shelf are normal-to-high compared with previous NW Mediterranean data (Table 4). Most of the radiometric analyses of shallow marine sediments in the NW Mediterranean Sea correspond to the Gulf of Lion (e.g. Radakovitch et al., 1999; Tateda et al., 2003; Miralles et al., 2005) although some studies have been carried out near Barcelona (see compilation in Fig. 9). Depositional rates in the Llobregat prodelta are smaller than those from largest rivers like the Amazon, the Yangtze or

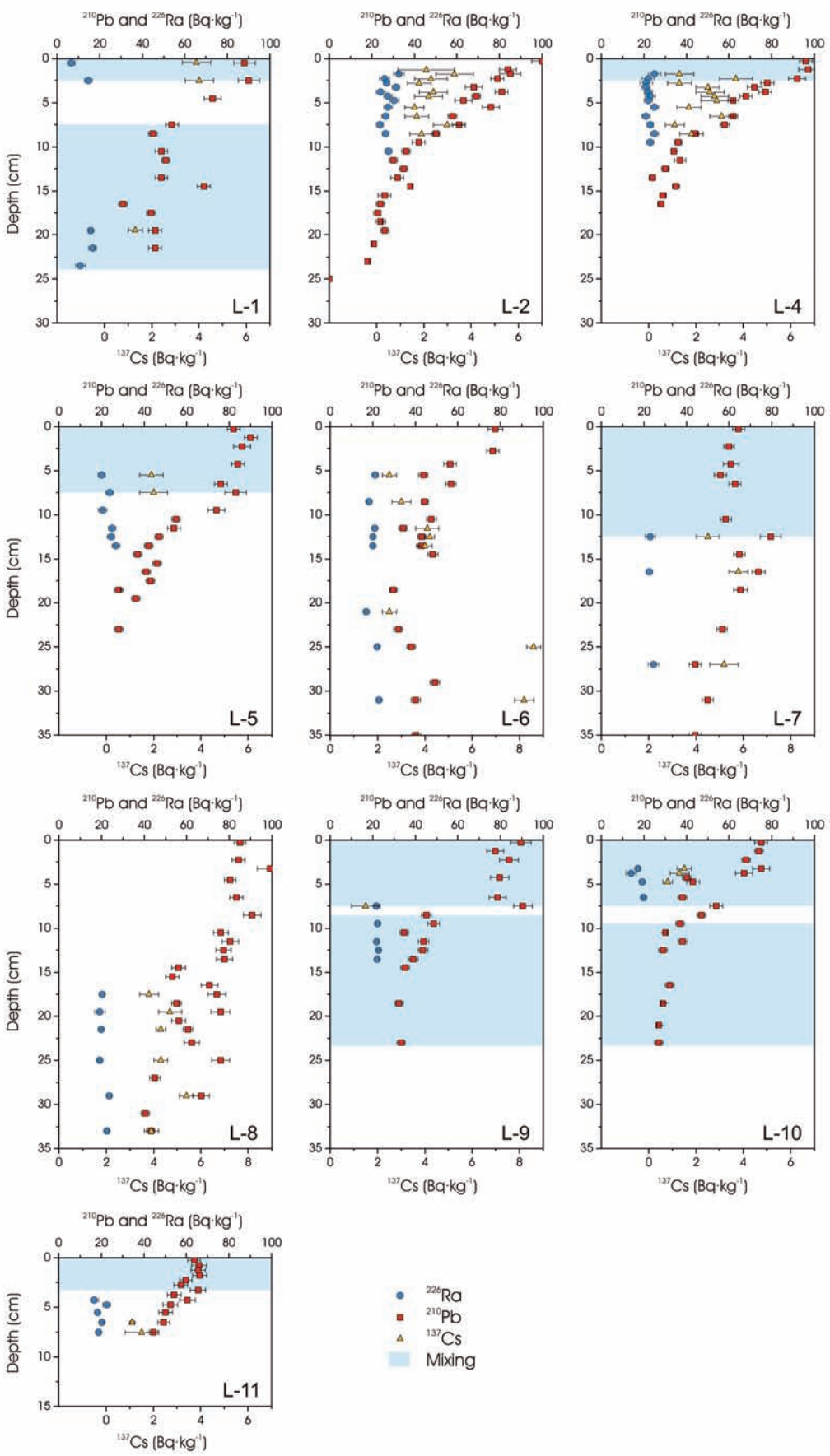
^{210}Pb and ^{226}Ra (Bq·kg^{-1})
Depth (cm)
^{137}Cs (Bq·kg^{-1})
L-1
L-2
L-4
L-5
L-6
L-7
L-8
L-9
L-10
L-11
^{226}Ra
^{210}Pb
^{137}Cs
Mixing

TABLE 3 | **Radiometric results and apparent accumulation rates of the sediment cores.**

Sediment core	Mixing depth (cm)	Surface ^{210}Pb activity (Bq·kg^{-1})	^{210}Pb at the core bottom (Bq·kg^{-1})	^{226}Ra (Bq·kg^{-1})	Apparent accum. rate (g·cm^{-2}·yr^{-1})	Apparent accum. rate (cm·yr^{-1})
L-1	> 23	87.8±4.8	41.7±7.0	14.5±2.5	—	—
L-2	0	99.6±5.1	26.9±2.5	27.6±2.7	0.24±0.01	0.20±0.01
L-4	2.5	96.2±3.0	29.3±4.5	22.8±1.5	0.21±0.02	0.16±0.02
L-5	7.5	82.0±2.9	27.8±0.5	24.5±2.5	0.21±0.01	0.17±0.01
L-6	0	77.6±3.4	40.7±9.2	20.3±2.0	1.03±0.28	0.80±0.21
L-7	12.5	64.4±2.8	46.0±3.4	23.3±1.1	0.70±0.21	0.64±0.17
L-8	0	85.0±2.7	43.1±2.0	20.8±1.9	0.94±0.04	1.00±0.04
L-9	> 23	89.5±4.9	33.6±1.5	22.1±0.4	—	—
L-10	7.5	74.7±2.9	29.3±1.7	19.6±3.2	—	—
L-11	3.5	63.6±3.1	44.6±2.1	19.3±2.2	0.46±0.12	0.36±0.09

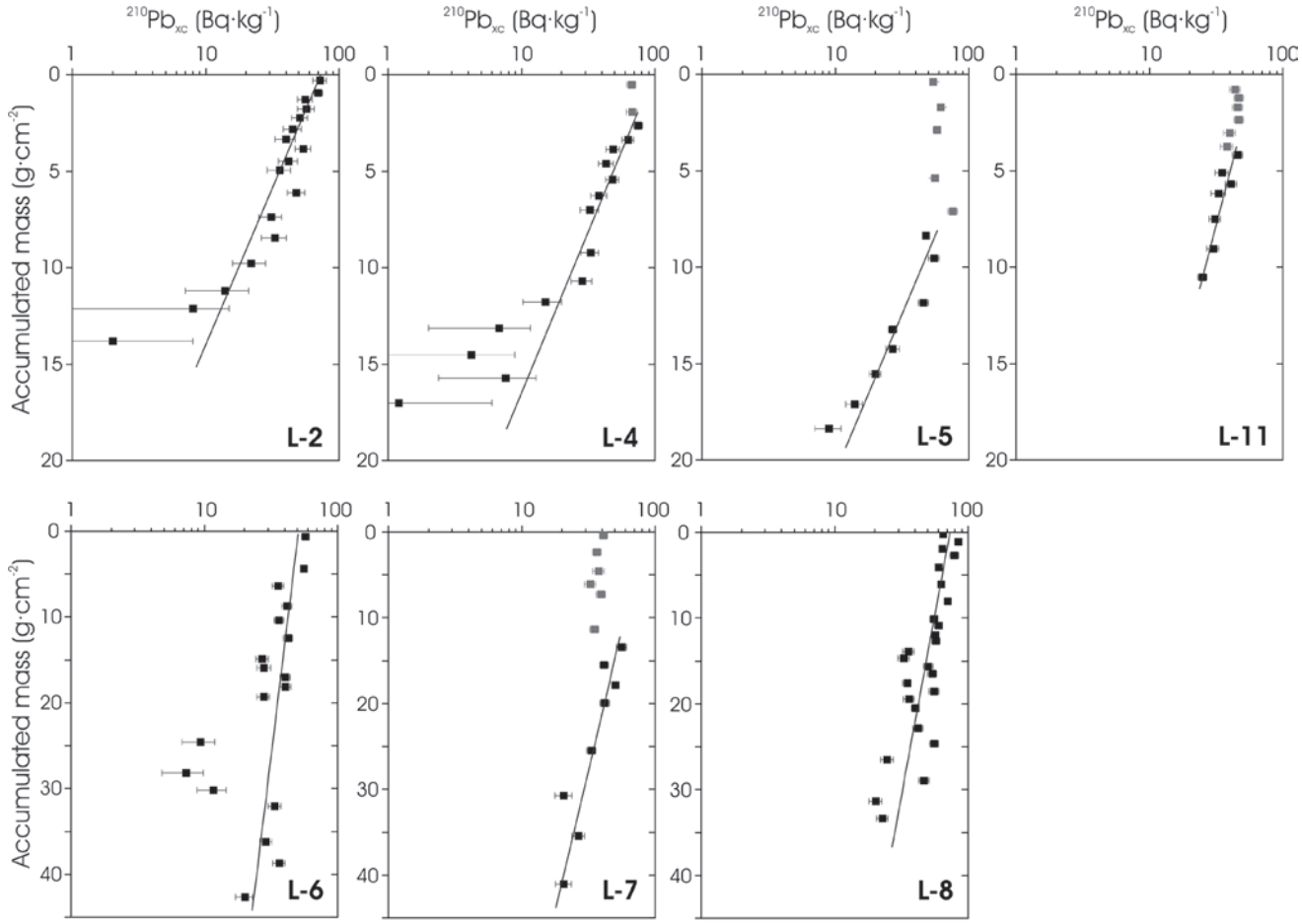

FIGURE 8 | **^{210}Pb excess activity data *versus* cumulative mass and the linear regressions used to estimate mass accumulation rates. Grey points correspond to mixed sediments and they are not taken into account for the linear regressions.**

the Po submarine deltas, where sediments may accumulate at a rate of up to 100 mm·yr^{-1} (Table 4). However, they are comparable with other worldwide continental shelves (Table 4).

Accumulation rates over continental margins usually decrease with depth and with the distance to major rivers and submarine canyon heads (e.g. Palanques et al., 1998; Radakovitch and Heussner, 1999; Sommerfield and Nittrouer, 1999; Lewis et al., 2002; Alexander and Venherm, 2003). In the Barcelona continental shelf, accumulation rates are particularly high near the Llobregat river mouth and tend to decrease offshore (with minor exceptions in cores "c" and L-11, see Fig. 9). These results confirm that the modern deposition is controlled by fluvial inputs and, in particular, by the major input of the Llobregat River. When the suspended sediment load carried by the Llobregat and Besòs rivers reaches the shelf, it is mostly deflected south-westward (alongshore) by the prevailing littoral drift and oceanographic currents, which are especially intense over the continental slope. Puig et al. (2000) stated that settling of suspended particles must be relatively low over the Barcelona continental slope due to advective processes. However, we find a moderate accumulation rate in site L-4, most probably influenced by the nearby Llobregat River and by the narrowness of the continental shelf on that position. An important part of the suspended material on the Barcelona continental shelf may become trapped by the Foix Canyon (Sanchez-Cabeza et al., 1999; Puig et al., 2000; Palanques et al., 2008), as evidenced by data shown in Figure 9.

HUMAN IMPACTS

Regression of the river-influenced depositional environment

River-influenced sediments were observed in the deeper part of core L-4 (between 5-17 cm below the seafloor). According to the estimated accumulation rate, core L-4 contains the sedimentary record of the last century going back to the end of 19th century. The observed change in sediment input occurred around 1966. The core section that contain river-derived sediments spans an age of about 70 years and, hence, it cannot be referred to an exceptional river flood or seafloor instability process (e.g. landslide, debris flow) that could allow the river-derived material to reach the upper slope. In addition, the ^{137}Cs chronology confirms the ^{210}Pb-decay accumulation rate, which indicates that only the top 2.5 cm of L-4 may be affected by mixing processes. We hypothesize that the change from river-derived to prevailing marine-derived sediments recorded in core L-4 responds to the first major enlargement of the port of Barcelona, as 1966 is the year when it was extended from its earlier northeastern position (the old port or "Port Vell") to the south of Montjuic hill ("M" in Fig. 1) through the building of an inner port that invaded a considerably long stretch of the Llobregat Delta (APB, 2003). The hardening of this part of the delta coast, and its likely effect on littoral drift and currents, would have caused the cessation of the arrival of river-derived inputs to the location of L-4. At present, off the Llobregat River, river-derived sediments do not accumulate beyond the outer shelf (site L-5). As a result, the offshore farthest boundary of river-derived sedimentation off the Llobregat outlet has receded 2.5 km after 1966.

Similarly, we observed a reduction of river-derived components in the upper interval of L-2, which is an undisturbed core. Only some micas and rare plant debris were observed in the upper 9 cm of this core. However, grain size, statistical parameters and compositional changes down-core (abundant large bioclasts and biogenic fragments) suggest a greater marine influence since about 1964. In the case of L-2, such a reduction in fluvial inputs could be linked not only to the extension of the Barcelona harbor but also to the increasing hardening of the Besòs coast and to the canalization of the lower river course after the catastrophic floods of 1962 (CLABSA, 2007).

Other factors that may have contributed to the regression of river-derived inputs and sedimentation are:

- Sediment retention in the Llobregat River reservoirs. Four dams placed in the upper course regulating 17.5% of the basin area were constructed in the Llobregat River between 1957 and 1999. These dams have a trapping efficiency of 74-97% that, related to their position within the watershed, translates into an effective trapping efficiency at the river mouth of 1.1-9.7% (Liquete et al., 2009).
- Sand and gravel mining from the Llobregat riverbed during the fifties and sixties. The open pits may have trapped substantial volumes of sediment coming from upstream.
- The rapid urbanization of the Llobregat Basin and Delta related to the expansion of the city of Barcelona and other surrounding towns, industrial areas and infrastructures.
- A significant decrease in the Besòs and Llobregat water discharge estimated in 0.6 and 3.4 m^3·s^{-1}, respectively, between 1960 and 2000 (Liquete, 2008).
- The decrease of river sedimentation agrees with Puchades (1948) and Marquès and Julià (1983) who warned about the severe regression of the Llobregat Delta since the mid-20th century. Recent data (EEA, 2005) demonstrate that most of the Llobregat Delta undergoes coastal recession.

TABLE 4 | **Modern sediment accumulation rates estimated through radiometric analyses in different worldwide continental shelves. C.S.= continental shelf. *: Compilation from different authors.**

Accumulation rate ($mm \cdot yr^{-1}$)	Physiographic province	Site location	Ocean margin	Reference
1.0-2.0	Middle C.S.	Ebro margin (NE Spain)	NW Mediterranean	Zuo et al., 1997
2.1-26.0	Prodelta area	Gulf of Lion (S France)	NW Mediterranean	Radakovitch et al., 1999
0.7-2.2	C.S.	Barcelona margin (NE Spain)	NW Mediterranean	Sanchez-Cabeza et al., 1999
1.5-1.8	Outer C.S.	Offshore Monaco (S France)	NW Mediterranean	Tateda et al., 2003
0.7-3.6	C.S.	Gulf of Lion (S France)	NW Mediterranean	Miralles et al., 2005*
2.0-6.5	Prodelta area	Gulf of Lion (S France)	NW Mediterranean	Miralles et al., 2005*
1.6-10	C.S.	Barcelona margin (NE Spain)	NW Mediterranean	This study
3.3-12.8	Subaqueous delta (26-65 m depth)	Gargano Promontory, Adriatic Sea	N Mediterranean	Cattaneo et al., 2003
0.2-16.4 (max. 48)	C.S. (6-238 m depth)	Western Adriatic Sea	N Mediterranean	Frignani et al., 2005*
1.1-20.2	C.S. (12-73 m depth)	Appennine Shelf, central Adriatic Sea	N Mediterranean	Palinkas and Nittrouer, 2006
2.3-46	Prodelta area (<25 m depth)	Po Shelf, northern Adriatic Sea	N Mediterranean	Palinkas and Nittrouer, 2007
1.0-2.7 (max. 5.6)	Mud fields on C.S. (30-75 m depth)	Gironde Shelf, Bay of Biscay (W France)	NE Atlantic	Lesueur et al., 2001
0.8-5.7	Semi-enclosed bay (<8 m depth)	Albemarle Estuary (North Carolina)	NW Atlantic	Corbett et al., 2007
<10-100	Prodelta area	Amazon Shelf (Brazil)	SW Atlantic	Kuehl et al., 1986
2.0-8.0	C.S. (50-150 m depth)	Eel Shelf (California)	NE Pacific	Sommerfield and Nittrouer, 1999
1.0-3.9	C.S. (10-130 m depth)	Monterey Bay (California)	NE Pacific	Lewis et al., 2002
0.9-12.8 (max. 51.9)	C.S. (<200m depth)	Santa Monica Bay (California)	NE Pacific	Alexander and Venherm, 2003
4.7-8.1	Middle C.S.	Eel Shelf (California)	NE Pacific	Bentley and Nittrouer, 2003
1.0-30.0	C.S.	Northern Gulf of Alaska	NE Pacific	Jaeger and Nittrouer, 2006
2.2-4.3	C.S. and upper slope (20-450 m depth)	Sagami Bay (Tokyo)	NW Pacific	Kato et al., 2003
10-50	Prodelta area	Yangtze Shelf, East China Sea	W Pacific	DeMaster et al., 1985
1.0-6.6	C.S. and upper slope (30-370 m depth)	Eastern Arabian Sea	NW Indic	Somayajulu et al., 1999

Mixing of seafloor sediments

Uniform ^{210}Pb activity profiles, as well as other homogeneous textural and physical characteristics, indicate that cores L-1, L-9 and L-10 are discontinuously but entirely disturbed. L-1 is located only 0.4 km far from the harbor's anchoring zone and 1.5 km far from the Port of Barcelona new enlargement area, which probably affected its sedimentation. The great impact of the enlargement works of the port of Barcelona has been evidenced by multibeam data (Liquete et al., 2007; Liquete, 2008). These works translate into dredging, loading and infilling that affect more than 5 km of shoreline and 2 km offshore. The bathymetric images show also clear evidences of ship anchoring as hollows that penetrate up to 70 cm within the sediment. Cores L-9 and L-10 are sited off the Llobregat River below the minimum trawling limit (50 m depth). Therefore, these cores may have been disturbed by trawling activities that are common in the study area (Liquete, 2008).

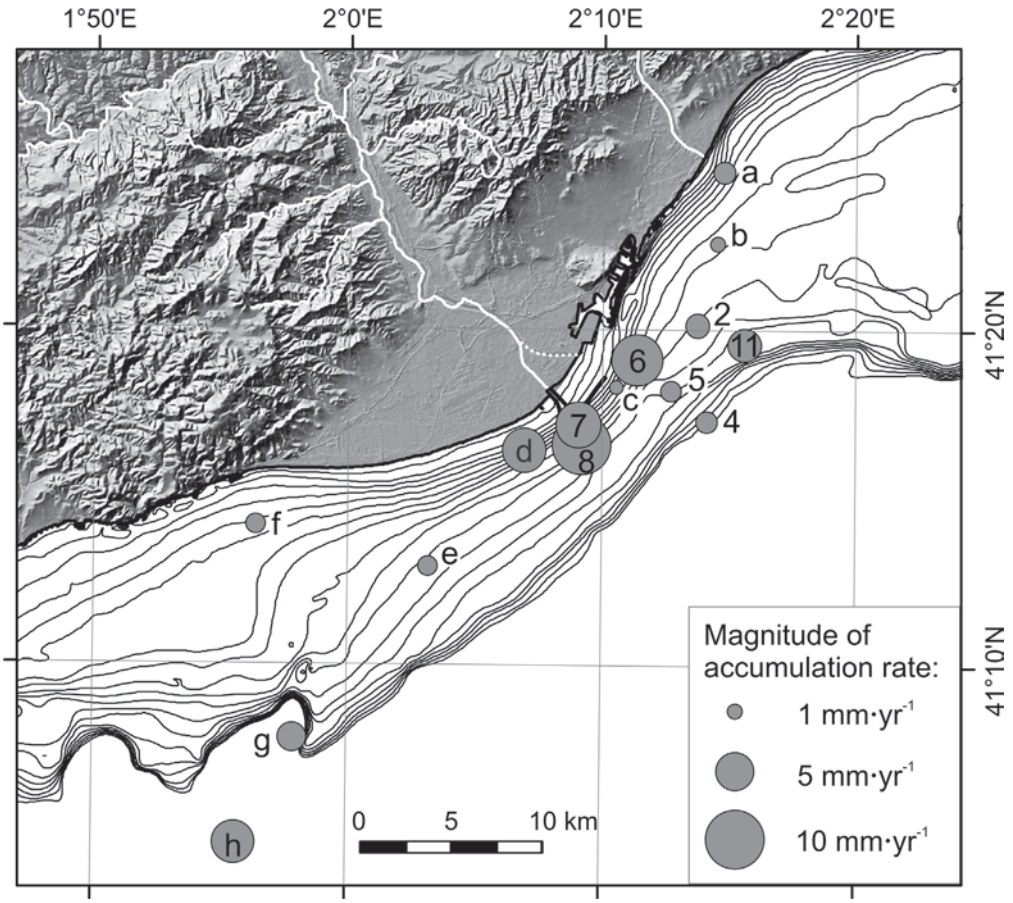

FIGURE 9 | **Sediment accumulation rates in the study area. Numbers refer to the cores analyzed in this study; a-b) after Palanques et al. (1998); c-h) after Sanchez-Cabeza et al. (1999). The dashed white line points to the Llobregat river mouth before 2004. Bathymetric contours every 10 m.**

Bottom trawling tracks are reflected in the multibeam images of the study area as parallel furrows <1 m deep (Liquete et al., 2007). Surface sediment re-suspension by trawling activities is responsible for an important increase in water column turbidity several meters above the sea bottom, and for important changes in the biogeochemical composition of the suspended particulate organic matter (Palanques et al., 2001; Pusceddu et al., 2005).

Apart from the entirely disturbed cores, the uppermost 2.5-12.5 cm of cores L-4, L-5, L-7 and L-11 seem to be mixed. The shallowest and most affected of these cores, L-7, is only 0.6 km far from the harbor's anchoring zone and 1.0 km far from the Port of Barcelona new enlargement area. In general, the surface mixed layer of the Barcelona continental shelf gets thinner with water depth. This surface sediment disturbance must be due to the human activities reported above, since the other possible origin, bioturbation, has a minor importance according to our observations.

We can conclude that, in the Barcelona continental shelf, (a) sea floor sediments can be intensively disturbed by human activities at least down to 85 m depth, and (b) a surface mixed layer is detected at least down to 150 m depth.

Possible organic contamination

Some authors (e.g. Hedges and Keil, 1995; Hedges et al., 1997) suggest that less than 1% of the OC delivered to the ocean is ultimately buried in marine sediments. Such a low preservation results, for instance, in marine sediments' OC concentrations of 0.8% (in weight percentage) near the Rhone river mouth decreasing offshore until 0.3-0.4% at 100 m depth (Aloisi et al., 1976); from 0.6% to 1.8% in the Gulf of Lion with maximum values off the Rhone and Petit-Rhone river mouths (Roussiez et al., 2006); 1% in flood layers of the Po River prodelta (Miserocchi et al., 2007); 0.3% as the mean OC concentration of the southern European continental margins (Seiter et al., 2004); and 1-1.5% in the Eel continental shelf (Sommerfield et al., 2007), which is considered one of the most OC-enriched areas of the Pacific Ocean (Seiter et al., 2004).

The provenance of OC in the Barcelona shelf environment can be attributed to several sources, which include phytoplankton and algae (marine origin), soil-derived organic matter and land plants' debris (continental origin), and sewage delivery (human origin).

The sediments ascribed to marine sedimentation on the outer Barcelona continental shelf contain in average 0.35% of OC that can be tentatively related to marine biological productivity. In contrast, the OC content recorded in the fine-grained Llobregat prodelta (up to 1.6% with an average of 1.3%) seems high compared with the abovementioned reference values. This relatively high OC concentration can be associated to natural continental inputs and/or to anthropogenic pollution dispersed through rivers' discharge, emissaries and pipelines in the surroundings of Barcelona. Since the Llobregat River is a medium-sized system with relatively low water and sediment discharge (Liquete et al., 2009), the OC content of the Llobregat prodelta may reflect at least moderate organic pollution. The polluted fluvial discharge together with direct inputs to the Barcelona shelf from two sewage treatment plants, "Sant Adrià del Besòs" and "El Prat de Llobregat", able to process a total volume of 945,000 m^3 per day, are the most likely source of the possible OC contamination on the Llobregat prodelta sediments. In particular, the "Sant Adrià del Besòs" submarine emissary is only 1 km far from site L-8.

Previous studies indicate that the Barcelona continental shelf receives an important input of inorganic pollutants, namely heavy metals, that augmented drastically during the twenties and the sixties due to industrial development and population increase (Palanques and Diaz, 1994; Palanques et al 1998; Sanchez-Cabeza et al., 1999). Moreover, Palanques et al. (2008) conclude that anthropogenic contamination is affecting, not only the littoral and the continental shelf, but also the adjacent continental slope through submarine canyons.

CONCLUSIONS

The Barcelona continental shelf is dominated by sediment inputs from the Besòs and Llobregat rivers, which during the Holocene built up a joint prodelta occupying 193 km^2. The fluvial material is characterized by clayey to sandy silt minerals with abundant plant debris, high organic carbon content (>1%), and a C/N ratio larger than 13. Backscatter and sedimentological data show two modern mud patches extending south-westward 6.5 and 13 km from the Besòs and Llobregat river mouths, respectively. The present river-derived sediment spreads beyond the prodelta limit, as far as the middle shelf off the Besòs River and the outer shelf off the Llobregat River. However, before 1966, the river-influenced environment reached at least the upper slope off the Llobregat River. The regression of the river-derived sedimentation (estimated in ~2.5 km in 40 years) was likely caused by the occupation of the southern coast of the Llobregat Delta by new port facilities and by the canalization of the Besòs lower course, amongst other factors. Sediment organic carbon contents up to 1.65% near the Llobregat river mouth may indicate, apart from high organic matter levels typical from prodeltaic areas, possible organic pollution derived from the fluvial discharge and/or from the emissaries of two sewage treatment plants.

To the north of the Llobregat River, over the middle and outer shelf, the Barcelona along-shelf currents prevent the accumulation of modern fluvial sediment. This area represents a marine-influenced environment characterized by medium silt to medium sand deposits, rich in large bioclasts (33-52% of calcium carbonate), with relatively low organic carbon content (<0.5%). Within this area, backscatter mosaics allow identifying relict bedforms and important seafloor impacts like the enlargement works of the Port of Barcelona. The highest backscatter values have been associated to the coarsest sediments of the study area after groundtruthing with sediment samples.

In general, accumulation rates and surface sediment disturbance decrease gradually with the distance to the Llobregat river mouth. Maximum accumulation rates (up to 10 $mm \cdot yr^{-1}$) are observed off the Llobregat River, near a large field of wavy bedforms. Moderate accumulation rates (1.6-3.6 $mm \cdot yr^{-1}$) are found in the middle and outer shelf between the Besòs and Llobregat rivers. Similar rates were estimated for the nearby Foix Canyon head, where a substantial amount of suspended sediment bypassing the Barcelona shelf seems to be trapped. Dredging, ship anchoring and trawling activities, especially intense off the Port of Barcelona down to 85 m depth, cause sediment mixing in the upper 2.5-24 cm of the sediments.

ACKNOWLEDGMENTS

The authors are grateful to the R/V "García del Cid" shipboard scientific party (Joan Manel Bruach, Eduard Costa, Manel García, Carolina Olid, Elisabet Verdeny and Diana Zúñiga) and crew for the collective effort during data collection. Montserrat Guart, Joan Manel Bruach and Diana Zúñiga are also thanked for technical support with sedimentological and geochemical analyses. This research was funded by the Spanish PRODELTA (REN2002-02323) and GRACCIE CONSOLIDER-INGENIO 2010 (ref. CSD2007-00067) projects. GRC Geociències Marines is funded by Generalitat de Catalunya grant SGR2005 00152 to excellence research groups. J. Garcia-Orellana acknowledges the Government of Spain and the Fulbright Commission for the concession the post-doctoral fellowship ref. 2007-0516.

REFERENCES

Alexander, C.R., Venherm, C., 2003. Modern sedimentary processes in the Santa Monica, California continental

margin: sediment accumulation, mixing and budget. Marine Environmental Research, 56(1-2), 177-204.

Aloisi, J.C., Cauwet, G., Gadel, F., Got, H., Monaco, A., Vile, F., Causse, C., Pagnon, M., 1976. Contribution à l'étude de la sedimentation récente et de la pollution sur le plateau continental du Golfe du Lion entre Fos-sur-Mer et Sète. Bulletin Bureau de Recherches Géologiques et Minières, 4(2), 69-83.

Amblas, D., Canals, M., Urgeles, R., Lastras, G., Liquete, C., Hughes-Clarke, J.E., Casamor, J.L., Calafat, A.M., 2006. Morphogenetic mesoscale analysis of the northeastern Iberian margin, NW Mediterranean Basin. Marine Geology, 234, 3-20.

Amorosi, A., 1995. Glaucony and sequence stratigraphy: a conceptual framework of distribution in siliciclastic sequences. Journal of Sedimentary Research, B65, 419-425.

APB (Autoritat Portuària de Barcelona), 2003. History of The Port. 1966: The expasion by the Delta. Available on-line: http://www.apb.es/en/APB/History/1966_Expansion_By_Delta.

Bentley, S.J., Nittrouer, C.A., 2003. Emplacement, modification, and preservation of event strata on a flood-dominated continental shelf: Eel shelf, Northern California. Continental Shelf Research, 23, 1465-1493.

Blondel, P., Murton, B.J., 1996. Handbook of Seafloor Sonar Imagery. Chichster (UK), John Wiley and Sons, 314pp.

Borgeld, J.C., Hughes-Clarke, J.E., Goff, J.A., Mayer, L.A., Curtis, J.A., 1999. Acoustic backscatter of the 1995 flood deposit on the Eel shelf. Marine Geology, 154, 197-210.

Bremner, J.M., Willis, J.P., 1993. Mineralogy and geochemistry of the clay fraction of sediments from the Namibian continental margin and the adjacent hinterland. Marine Geology, 115, 85-116.

Canals, M., Casamor, J.L., Urgeles, R., Farrán, M., Calafat, A.M., Amblas, D., Willmott, V., Estrada, F., Sánchez, A., Arnau, P., Frigola, J., Colàs, S., 2004. Mapa del relleu submarí de Catalunya. 1:250000. Institut Cartogràfic de Catalunya, Barcelona.

Castellón, A., Font, J., García, E., 1990. The Liguro-provençal-Catalan current (NW Mediterranean) observed by Doppler profiling in the Baleary Sea. Scientia Marina, 54, 269-276.

Cattaneo, A., Correggiari, A., Langone, L., Trincardi, F., 2003. The late-Holocene Gargano subaqueous delta, Adriatic shelf: Sediment pathways and supply fluctuations. Marine Geology, 193(1-2), 61-91.

CLABSA (Clavegueram de Barcelona S.A.), 2007. Parc Fluvial del Besòs. La canalització del riu Besòs. Available on-line: http://www.clabsa.es/CAT/ParcFluvial_Canalitzacio.asp, last revision in July 2007.

Collier, J.S., Brown, C.J., 2005. Correlation of sidescan backscatter with grain size distribution of surficial seabed sediments. Marine Geology, 214(4), 431-449.

Corbett, D.R., Vance, D., Letrick, E., Mallinson, D., Culver, S., 2007. Decadal-scale sediment dynamics and environmental change in the Albemarle Estuarine System, North Carolina. Estuarine, Coastal and Shelf Science, 71(3-4), 717-729.

DeMaster, D.J., McKee, B.A., Nittrouer, C.A., Qian, J., Cheng, G., 1985. Rates of sediment accumulation and particle reworking based on radiochemical measurements from continental shelf deposits in the East China Sea. Continental Shelf Research, 4, 143-158.

Dounas, C., Davies, I., Triantafyllou, G., Koulouri, P., Petihakis, G., Arvanitidis, C., Sourlatzis, G., Eleftheriou, A., 2007. Large-scale impacts of bottom trawling on shelf primary productivity. Continental Shelf Research, 27(17), 2198-2210.

Edwards, B.D., Dartnell, P., Chezar, H., 2003. Characterizing benthic substrates of Santa Monica Bay with seafloor photography and multibeam sonar imagery. Marine Environmental Research, 56, 47-66.

EEA (European Environment Agency), 2005. EUROSION dataset: Geomorphology, Geology, Erosion trends and Coastal defence works. Available on-line: http://dataservice.eea.europa.eu/dataservice/metadetails.asp?id=730, last revision in February 2005.

Emerson, S., Hedges, J.I., 1988. Processes controlling the organic carbon content of open ocean sediments. Paleoceanography, 3, 621-634.

European Communities, 2000. The Urban Audit. Towards the Benchmarking of Quality of Life in 58 European Cities. Luxembourg, Office for Official Publications of the European Communities, II, 239pp. Available on-line: http://ec.europa.eu/regional_policy/urban2/urban/audit/src/yearbook.htm.

Fernández-Bastero, S., Gago-Duport, L., García, T., Velo, A., Santos, A., Vilas, F., 2001. Condiciones geoquímicas para la formación y maduración de minerales glauconíticos. In: Lago, M., Arranz, E., Galé, C. (eds.). Zaragoza, 23-26/10/2001, Proceedings, III Iberian Geochemistry Meeting and VIII Geochemistry Meeting of Spain, 439-442.

Flexas, M.M., Durrieu de Madron, X., García, M.A., Canals, M., Arnau, P., 2002. Flow variability in the Gulf of Lions during the MATER HFF experiment (March-May 1997). Journal of Marine Systems, 33-34, 197-214.

Font, J., García-Ladona, E., Górriz, G. E., 1995. The seasonality of mesoscale motion in the Northern Current of the western Mediterranean: several years of evidence. Oceanologica Acta, 18, 207-219.

Friedman, G.M., 1967. Dynamic processes and statistical parameters compared for size frequency distribution of beach and river sands. Journal of Sedimentary Petrology, 37, 327-354.

Frignani, M., Langone, L., Ravaioli, M., Sorgente, D., Alvisi, F., Albertazzi, S., 2005. Fine-sediment mass balance in the western Adriatic continental shelf over a century time scale. Marine Geology, 222-223, 113-133.

Gao, S., Ping Wang, Y., 2008. Changes in material fluxes from the Changjiang River and their implications on the adjoining continental shelf ecosystem. Continental Shelf Research, 28(12), 1490-1500.

Goff, J.A., Olson, H.C., Duncan, C.S., 2000. Correlation of side-scan backscatter intensity with grain-size distribution of shelf sediments, New Jersey margin. GeoMarine Letters, 20, 43-49.

Goldberg, E.D., 1963. Geochronology with ^{210}Pb. In: International Atomic Energy Agency (eds.). Radioactive dating. Vienna, International Atomic Energy Agency (IAEA), 121-131.

Hartwell, S.I., 2008. Distribution of DDT and other persistent organic contaminants in Canyons and on the continental shelf off the central California coast. Marine Environmental Research, 65(3), 199-217.

Hedges, J.I., Keil, R.G., 1995. Sedimentary organic matter preservation: an assessment and speculative synthesis. Marine Chemistry, 49, 81-115.

Hedges, J.I., Keil, R.G., Benner, R., 1997. What happens to terrestrial organic matter in the ocean? Organic Geochemistry, 27, 195-212.

ITGE (Instituto Tecnológico GeoMinero de España), 1989. Mapa Geológico de la Plataforma Continental Española y Zonas Adyacentes. Madrid, escala 1:200000, memoria y hoja 35-42A (Barcelona), 117pp.

Jaeger, J.M., Nittrouer, C.A., 2006. A quantitative examination of modern sedimentary lithofacies formation on the glacially influenced Gulf of Alaska continental shelf. Continental Shelf Research, 26(17-18), 2178-2204.

Kato, H., Kitazao, H., Shimanaga, M., Nakatsuka, T., Shirayama, Y., Masuzawa, T., 2003. ^{210}Pb and ^{137}Cs in sediments from Sagami Bay: sedimentation rates and inventories. Progress in Oceanography, 57, 77-95.

Kuehl, S.A., DeMaster, D.J., Nittrouer, C.A., 1986. Nature of sediment accumulation on the Amazon continental shelf. Continental Shelf Research, 6, 209-225.

Lesueur, P., Jouanneau, J.M., Boust, D., Tastet, J.P., Weber, O., 2001. Sedimentation rates and fluxes in the continental shelf mud fields in the Bay of Biscay (France). Continental Shelf Research, 21(13-14), 1383-1401.

Lewis, R.C., Coale, K.H., Edwards, B.D., Marot, M., Douglas, J.N., Burton, E.J., 2002. Accumulation rate and mixing of shelf sediments in the Monterey Bay National Marine Sanctuary. Marine Geology, 181(1-3), 157-169.

Liquete, C., 2008. The Barcelona continental shelf: Source to Sink analysis and anthropogenic impacts. Doctoral Thesis. Barcelona (Spain), University of Barcelona, 276pp.

Liquete, C., Canals, M., Lastras, G., Amblas, D., Urgeles, R., De Mol, B., De Batist, M., Hughes-Clarke, J.E., 2007. Long-term development and current status of the Barcelona continental shelf: A source-to-sink approach. Continental Shelf Research, 27(13), 1779-1800.

Liquete, C., Canals, M., De Mol, B., De Batist, M., Trincardi, F., 2008. Quaternary stratal architecture of the Barcelona prodeltaic continental shelf (NW Mediterranean). Marine Geology, 250(3-4), 234-250.

Liquete, C., Canals, M., Ludwig, W., Arnau, P., 2009. Sediment discharge of the rivers of Catalonia, NE Spain, and the influence of human impacts. Journal of Hydrology, 366, 76-88.

Logvinenko, N.V., 1982. Origin of glauconite in the recent bottom sediments of the ocean. Sedimentary Geology, 31, 43-48.

Manzano, M., 1986. Estudio sedimentológico del prodelta holoceno del Llobregat. MScThesis. Barcelona (Spain), University of Barcelona, 150pp.

Marquès, M.A., 1974. Las formaciones cuaternarias del delta del Llobregat. Doctoral Thesis. Barcelona (Spain), University of Barcelona, 401pp.

Marquès, M.A., Julià, R., 1983. Coastal problems in Alt Emporadá Area (NE Catalonia, Spain). In: Bird, E.C.F., Fabbri, P. (eds.). Coastal Problems in Mediterranean Sea. International Geographical Union (IGU), Bologna, Commission on the Coastal Environment, 83-93.

McLaren, P., Boweles, D., 1985. The effects of sediment transport on grain size distributions. Journal of Sedimentary Petrology, 55, 457-470.

Meyers, P.A., 1994. Preservation of elemental and isotopic source identification of sedimentary organic matter. Chemical Geology, 114(3-4), 289-302.

Millot, C., 1999. Circulation in the Western Mediterranean Sea. Journal of Marine Systems, 20, 423-442.

Miralles, J., Radakovitch, O., Aloisi, J.-C., 2005. ^{210}Pb sedi–mentation rates from the Northwestern Mediterranean margin. Marine Geology, 216(3), 155-167.

Miserocchi, S., Langone, L., Tesi, T., 2007. Content and isotopic composition of organic carbon within a flood layer in the Po River prodelta (Adriatic Sea). Continental Shelf Research, 27(3-4), 338-358.

Nelsen, T.A., Blackwelder, P., Hood, T., McKee, B., Romer, N., Alvarez-Zarikian, C., Metz, S., 1994. Time-based correlation of biogenic, lithogenic and authigenic sediment components with anthropogenic inputs in the Gulf of Mexico NECOP study area. Estuaries, 17(4), 873-885.

Nieuwenhuize, J., Maas, Y.E.M., Middelburg, J.J., 1994. Rapid analysis of organic carbon and nitrogen in particulate materials. Marine Chemistry, 45(3), 217-224.

Nitsche, F.O., Bell, R., Carbotte, S.M., Ryan, W.B.F., Flood, R., 2004. Process-related classification of acoustic data from the Hudson River Estuary. Marine Geology, 209, 131-145.

Odin, G.S. (ed.), 1988. Green Marine Clays. Oolitic Ironstone Facies, Verdine Facies, Glaucony Facies and Celadonite-Bearing Rock Facies - A Comparative Study. Elsevier (Ams–terdam), Developments in Sedimentology, 45, 446pp.

Odin, G.S., Matter, A., 1981. De glauconiarum origine. Sedimentology, 28, 611-641.

Palanques, A., Díaz, J.I., 1994. Anthropogenic heavy metal pollution in the sediment of the Barcelona continental shelf. Marine Environmental Research, 38, 17-31.

Palanques, A, Sanchez-Cabeza, J.A., Masqué, P., León, L, 1998. Historical record of heavy metals in a highly contaminated Mediterranean deposit: The Besós prodelta. Marine Chemistry, 61, 209-217.

Palanques, A., Guillén, J., Puig, P, 2001. Impact of bottom trawling on water turbidity and muddy sediment of an unfished continental shelf. Limnology and Oceanography, 46(5), 1100-1110.

Palanques, A., Masqué, P., Puig, P., Sanchez-Cabeza, J.A., Frignani M., Alvisi, F., 2008. Anthropogenic trace metals in the sedimentary record of the Llobregat continental shelf and adjacent Foix Submarine Canyon (northwestern Mediterranean). Marine Geology, 248(3-4), 213-227.

Palinkas, C.M., Nittrouer, C.A., 2006. Clinoform sedimentation along the Apennine shelf, Adriatic Sea. Marine Geology, 234(1-4), 245-260.

Palinkas, C.M., Nittrouer, C.A., 2007. Modern sediment accumulation on the Po shelf, Adriatic Sea. Continental Shelf Research, 27, 489-505.

Pettijohn, F.J., Potter, P.E., Siever, R., 1987. Sand and sandstone (2nd edition). New York, Springer-Verlag, 553pp.

Puchades, J.M., 1948. El río Besós. Estudio monográfico de hidrología fluvial. Publicaciones del Instituto Geológico, Diputación Provincial de Barcelona. Miscelanea Almera, 7(II), 195-354.

Puig, P., Palanques, A., 1998. Nepheloid structure and hydrographic control on the Barcelona continental margin, northwestern Mediterranean. Marine Geology, 149, 39-54.

Puig, P., Palanques, A., Sanchez-Cabeza, J.A., Masqué, P., 1999. Heavy metals in particulate matter and sediments in the southern Barcelona sedimentation system (North-western Mediterranean). Marine Chemistry, 63, 311-329.

Puig, P., Palanques, A., Guillén, J., García-Ladona, E., 2000. Deep slope currents and suspended particle fluxes in and around the Foix submarine canyon (NW Mediterranean). Deep-Sea Research I, 47, 343-366.

Pusceddu, A., Grémare, A., Escoubeyrou, K., Amouroux, J.M., Fiordelmondo, C., Danovaro, R., 2005. Impact of natural (storm) and anthropogenic (trawling) sediment resuspension on particulate organic matter in coastal environments. Continental Shelf Research, 25, 2505-2520.

Radakovitch, O., Heussner, S., 1999. Fluxes and budget of ^{210}Pb on the continental margin of the Bay of Biscay (Northeastern Atlantic). Deep-Sea Research II, 46, 2175-2203.

Radakovitch, O., Charmasson, S., Arnaud, M., Bouisset, P., 1999. ^{210}Pb and caesium accumulation in the Rhone delta sediments. Estuarine Coastal and Shelf Science, 48, 77-92.

Rao, V.P., Lamboy, M., Dupeuble, P.A., 1993. Verdine and other associated authigenic (glaucony, phosphate) facies from the surficial sediments of southwestern continental margin of India. Marine Geology, 111, 133-158.

Roussiez, V., Ludwig, W., Monaco, A., Probst, J.-L., Bouloubassi, I., Buscail, R., Saragoni, G., 2006. Sources and sinks of sediment-bound contaminants in the Gulf of Lions (NW Mediterranean Sea): A multi-tracer approach. Continental Shelf Research, 26, 1843-1857.

Rubio, A., Arnau, P.A., Espino, M., Flexas, M.M., Jordà, G., Salat, J., Puigdefàbregas, J., Arcilla, A.S., 2005. A field study of the behaviour of an anticyclonic eddy on the Catalan continental shelf (NW Mediterranean). Progress in Oceanography, 66, 142-156.

Sanchez-Cabeza, J.A., Masqué, P., Ani-Ragolta, I., 1998. ^{210}Pb and ^{209}Po analysis in sediments and soils by microwave acid digestion. Journal of Radioanalytical and Nuclear Chemistry, 227, 19-22.

Sanchez-Cabeza, J.A., Masqués, P., Ani-Ragolta, I., Merino, J., Frignani, M., Alvisi, F., Palanques, A, Puig, P., 1999. Sediment accumulation rates in the southern Barcelona continental margin (NW Mediterranean Sea) derived from ^{210}Pb and ^{137}Cs chronology. Progress in Oceanography, 44, 313-332.

Seiter, K., Hensen, C., Schroter, J., Zabel, M., 2004. Organic carbon content in surface sediments-defining regional provinces. Deep Sea Research I, 51(12), 2001-2026.

Shepard, F.P., 1954. Nomenclature based on sand-silt-clay ratios. Journal of Sedimentary Petrology, 24, 151-158.

Somayajulu, B.L.K., Rhushan, R., Sarkar, A., Burr, G.S., Jull, A.J.T., 1999. Sediment deposition rates on the continental margins of the eastern Arabian Sea using ^{210}Pb, ^{137}Cs and ^{14}C. Science of the Total Environment, 237, 429-439.

Sommerfield, C.K., Nittrouer, C.A., 1999. Modern accumulation rates and a sediment budget for the Eel shelf: a flood-dominated depositional environment. Marine Geology, 154(1-4), 227-241.

Sommerfield, C.K., Ogston, A.S., Mullenbach, B.L., Drake, D.E., Alexander, C.R., Nittrouer, C.A., Borgeld, J.C., Wheatcroft, R.A., Leithold, E.L., 2007. Oceanic dispersal and accumulation of river sediment. In: Nittrouer, C.A., Austin, J.A., Field, M.E., Kravitz, J.H., Syvitski, J.P.M., Wiberg, P.L. (eds.). Continental Margin Sedimentation: From Sediment Transport to Sequence Stratigraphy. Blackwell Publishing, Malden, International Association of Sedimentologists (IAS), 37(Special Publication), 157-212.

Stein, R., 1991. Accumulation of organic carbon in marine sediments. Lecture Notes on Earth Science, Universität Giessen, Springer Verlag, 34, 217pp.

Sutherland, R.A., Lee, C.-T., 1994. Discrimination between coastal subenvironments using textural characteristics. Sedimentology, 41, 1133-1145.

Sutherland, T.F., Galloway, J., Loschiavo, R., Levings, C.D., Hare, R., 2007. Calibration techniques and sampling resolution requirements for groundtruthing multibeam acoustic backscatter (EM3000) and QTC VIEW™ classification technology. Estuarine, Coastal and Shelf Science, 75, 447-458.

Tateda, Y., Carvalho, F.P., Fowler, S.W., Miquel, J.-C., 2003. Fractionation of ^{210}Po and ^{210}Pb in coastal waters of the NW Mediterranean continental margin. Continental Shelf Research, 23(3-4), 295-316.

Urgeles, R., Locat, J., Schmitt, T., Hughes-Clarke, J.E., 2002. The July 1996 flood deposit in the Saguenay Fjord, Quebec, Canada: implications for sources of spatial and temporal backscatter variations. Marine Geology, 184, 41-60.

Urgeles, R., De Mol, B., Liquete, C., Canals, M., De Batist, M., Hughes-Clarke, J.E., Arraix Shipboard Party, 2007. Sediment undulations on the Llobregat prodelta: Signs of early slope instability or sedimentary bedforms? Journal of Geophysical Research, 112, B05102.

Visher, G.S., 1969. Grain size distribution and depositional processes. Journal of Sedimentary Petrology, 9, 1074-1106.

Zuo, Z., Eisma, D., Gieles, R., Besks, J., 1997. Accumulation rates and sediment deposition in the Northwestern Mediterranean. Deep-Sea Research II, 44, 597-609.

Manuscript received November 2008;
revision accepted May 2009;
published Online January 2010.

APPENDIX

TABLE I | **Grain size results (in weight percentage) and textural statistical parameters. VF= very fine; F= fine; M= medium; C= coarse; S.D.= standard deviation.**

APPENDIX

	GRAIN SIZE RESULTS (%)										TEXTURAL STATISTICAL PARAMETERS		
Sample	clay	VF silt	F silt	M silt	C silt	VF sand	F sand	M sand	C sand	>1 mm	Mean	S.D.	Skew-ness
Core L-1													
0-1 (cm)	21.04	15.66	22.26	17.92	16.33	6.68	0.13	0	0	0	11.78	3.40	-0.30
2-3	22.32	16.21	21.9	17.46	15.77	6.17	0.18	0	0	0	11.28	3.39	-0.23
4-5	21.1	15.51	21.72	17.67	16.99	6.7	0.29	0	0	0	11.95	3.43	-0.28
6-7	25.13	18.69	24.05	17.61	14.04	0.48	0	0	0	0	9.15	3.03	-0.30
9-10	17.51	12.57	17.29	18.95	29.26	4.42	0	0	0	0	14.71	3.34	-0.65
12-13	23.71	16.82	22.93	19.09	17.21	0.24	0	0	0	0	9.89	3.11	-0.42
15-16	29.4	21.95	24.85	14.15	8.97	0.68	0	0	0	0	7.62	2.89	-0.12
18-19	26.3	19.65	24.48	15.76	11.35	2.45	0	0	0	0	8.80	3.10	-0.16
21-22	29.33	21.26	25.2	15.41	8.75	0.04	0	0	0	0	7.56	2.86	-0.22
23-24	23.86	18.36	24.71	16.27	12.18	3.89	0.69	0	0	0	9.83	3.27	-0.14
averages	*23.97*	*17.67*	*22.94*	*17.03*	*15.09*	*3.18*	*0.13*	*0*	*0*	*0*	*10.26*		
Core L-2													
0-0.5 (cm)	14.26	10.54	17.74	19.29	25.56	11.17	0.73	0	0	0.68	18.18	3.59	-0.42
1-1.5	11.62	8.42	13.37	13.42	17.54	12.05	11.21	7.1	3.64	1.62	35.28	5.40	-0.13
2-2.5	13.2	9.27	15.09	15.28	17.94	11.88	10.41	4.89	0.56	1.46	27.33	4.93	-0.12
4-4.5	9.96	7.35	11.97	12.15	16.29	11.57	12.59	9.78	5.31	3.04	46.10	5.79	-0.21
6-7	14.78	11.29	17.76	16.91	18.71	8.86	4.64	4.48	0.75	1.82	21.68	4.75	0.16
8-9	13.44	10.3	16.85	16.93	19.62	7.69	4.53	5.03	4.08	1.56	25.42	5.15	0.20
10-11	19.34	14.24	19.76	16.13	16.93	8.72	0.25	0	0	4.61	15.82	4.70	0.55
14-15	22.48	16.35	21.36	15.8	15	7.65	0.23	0	0	1.12	11.96	3.80	0.20
18-19	24.17	17.72	22.36	15.31	10.91	5.06	2.96	0	0	1.49	11.25	4.00	0.48
22-24	22.6	15.7	21.69	16.7	12.11	5.28	1.28	0	0	4.62	13.15	4.80	0.72
averages	*16.59*	*12.12*	*17.8*	*15.79*	*17.06*	*8.99*	*4.88*	*3.13*	*1.43*	*2.2*	*22.62*		
Core L-4													
0-0.5 (cm)	18.26	11	15.23	12.1	11.18	19.01	13.25	0	0	0	20.81	4.86	-0.38
1-1.5	14.63	8.71	11.68	9.51	10.93	18.5	23.04	2.53	0.5	0	32.22	5.30	-0.56
2-2.5	21.46	12.48	16.49	12.33	10.44	15.82	11.02	0	0	0	16.92	4.85	-0.20
4-4.5	21.38	12.87	17.33	12.92	11.49	15.62	8.37	0	0	0	15.97	4.64	-0.19
6-7	28.05	16.48	20.61	14.03	6.25	7.76	6.85	0	0	0	10.58	4.26	0.20
10-11	28.82	18.09	22.86	15.13	8.22	4.79	2.07	0	0	0	8.78	3.62	0.07
14-15	26.25	15.79	19.37	12.05	7.45	8.43	9.83	0.81	0	0	12.45	4.80	0.18
16-17	32.05	18.59	21.79	11.97	5.38	7.99	2.2	0	0	0	8.36	3.85	0.26
averages	*23.86*	*14.25*	*18.17*	*12.51*	*8.92*	*12.24*	*9.58*	*0.42*	*0.06*	*0*	*15.76*		
Core L-5													
0-0.5 (cm)	18.96	13.94	19.24	16.31	17.51	10.4	3.65	0	0	0	14.86	3.80	-0.22
2-2.5	19.01	13.66	19.87	17.32	17.38	9.18	3.65	0	0	0	14.48	3.78	-0.25
4-4.5	17.97	13.22	18.1	15.31	16.99	10.44	7.26	0.42	0.3	0	17.05	4.16	-0.12
6-7	21.35	15.4	22.1	18.17	15.64	6.64	0.67	0	0	0	11.77	3.47	-0.27
10-11	23.02	17.15	22.93	16.91	13.54	5.93	0.55	0	0	0	10.74	3.39	-0.15
14-15	29.22	21.98	26.17	14.46	7.44	0.7	0	0	0	0	7.46	2.85	-0.17
18-19	27.81	20.87	25.13	15.38	8.58	2.25	0.02	0	0	0	8.16	3.00	-0.09
22-24	27.06	19.44	23.56	14.69	8.72	4.89	1.6	0	0	0	9.13	3.41	0.10
averages	*23.05*	*16.96*	*22.14*	*16.07*	*13.23*	*6.3*	*2.17*	*0.05*	*0.04*	*0*	*11.71*		
Core L-6													
0-0.5 (cm)	11.03	8.34	13.3	13.07	17.13	16.9	16.89	2.28	0.68	0.42	32.43	4.55	-0.45
2.5-3	10.17	7.67	12.85	13.47	17.81	17.38	16.76	3.1	0.61	0.17	34.17	4.43	-0.52
4-4.5	9.63	7.3	11.85	11.54	14.86	16.08	20.43	5.63	1.2	1.45	41.97	4.95	-0.46
6-7	12.08	9.08	14.04	12.74	15.59	15.35	15.91	3.88	1.02	0.31	31.08	4.83	-0.34
10-11	14.22	10.68	15.98	13.72	16.9	11.48	10.68	3.05	0.73	2.56	25.72	5.14	0.01
14-15	14.53	11.28	17.44	14.87	14.77	9.59	10.94	3.94	0.84	1.86	24.21	5.11	0.06
18-19	14.16	10.83	15.37	10.67	10.27	10.82	15.27	5.93	2.28	4.38	32.99	6.31	0.00
22-23	16.48	12.06	16.83	12.87	12.93	11.64	12.23	2.69	1.1	1.14	22.68	5.18	0.01
28-30	24.68	18.55	25.94	16.91	10.31	3.13	0.16	0	0	0.31	9.28	3.24	-0.02
34-36	25.57	18.75	24.8	16.38	10.94	3.32	0.02	0	0	0.21	9.10	3.27	-0.08
averages	*15.25*	*11.45*	*16.84*	*13.62*	*14.15*	*11.57*	*11.93*	*3.05*	*0.85*	*1.28*	*26.36*		

TABLE I | **Continue.**

	GRAIN SIZE RESULTS (%)										TEXTURAL STATISTICAL PARAMETERS		
Sample	**clay**	**VF silt**	**F silt**	**M silt**	**C silt**	**VF sand**	**F sand**	**M sand**	**C sand**	**>1 mm**	**Mean**	**S.D.**	**Skew-ness**
Core L-7													
0-0.5 (cm)	16.58	11.27	16.7	15.15	18.47	20.43	1.41	0	0	0	18.37	3.92	-0.48
2-2.5	13.12	9.61	13.87	12.28	16.8	22.6	11.73	0	0	0	26.27	4.22	-0.59
4-4.5	13.58	10.22	14.92	13.35	18.09	22.38	7.45	0	0	0	23.62	4.06	-0.55
6-7	13.65	9.99	14.42	12.63	15.79	19.92	13.51	0.04	0	0	25.56	4.35	-0.50
10-11	13.11	9.67	14.44	13.05	16.27	20.41	13.03	0.03	0	0	25.97	4.28	-0.53
14-15	18.19	14.09	20.86	17.41	22.56	6.84	0	0	0	0	13.66	3.37	-0.46
18-19	15.74	11.26	15.78	15.52	21.4	13.73	5.32	0.59	0.68	0	19.79	4.11	-0.31
22-24	15.53	11.17	16.54	15.38	20.39	16.08	4.86	0	0	0	19.30	3.93	-0.46
28-30	22.86	16.54	22.18	17.35	14.83	6.14	0.1	0	0	0	10.94	3.39	-0.23
34-36.5	22.91	16.69	22.69	16.52	14.16	6.81	0.04	0	0	0.13	10.93	3.46	-0.15
averages	*16.53*	*12.05*	*17.24*	*14.86*	*17.88*	*15.53*	*5.75*	*0.07*	*0.07*	*0.01*	*19.44*		
Core L-8													
0-0.5 (cm)	18.94	14.34	20.61	16.94	16.96	7.78	3.24	0.53	0.65	0	14.46	3.88	-0.03
2-2.5	20	15.5	22.67	18.24	17.1	6.47	0.04	0	0	0	12.08	3.35	-0.35
4-4.5	20.36	15.57	22.11	17.66	17.31	6.94	0.04	0	0	0	12.11	3.39	-0.33
6-7	20.68	16.33	24.14	18.79	16.22	3.82	0	0	0	0	11.12	3.20	-0.37
10-11	23.34	17.75	23.66	17.58	15.53	2.13	0	0	0	0	10.05	3.13	-0.28
14-15	23.77	18.79	25.11	18.28	13.23	0.79	0	0	0	0	9.40	2.97	-0.31
18-19	26.28	17.81	22.84	16.64	14.41	2.04	0	0	0	0	9.19	3.25	-0.25
22-24	22.64	17.15	24.26	18.97	14.23	2.75	0	0	0	0	10.18	3.14	-0.33
28-30	24.74	18.26	25.78	18.94	11.91	0.39	0	0	0	0	8.91	3.02	-0.41
32-34	24.5	18.54	24.31	16.6	12.08	3.95	0.02	0	0	0	9.60	3.19	-0.17
averages	*22.53*	*17*	*23.55*	*17.86*	*14.9*	*3.71*	*0.33*	*0.05*	*0.06*	*0*	*10.71*		
Core L-9													
0-0.5 (cm)	21.49	15.38	22.75	19.05	16.46	4.89	0	0	0	0	11.33	3.31	-0.36
1-1.5	20.57	15.81	23.27	18.72	16.53	5.14	0	0	0	0	11.55	3.27	-0.36
2-2.5	22.07	15.81	22.59	17.57	15.49	6.21	0.04	0	0	0.23	11.36	3.45	-0.17
4-4.5	21.79	16.35	23.2	18.03	15.33	5.31	0.02	0	0	0	11.06	3.31	-0.30
6-7	23.21	17.99	24.12	17.22	14.31	3.15	0	0	0	0	10.06	3.16	-0.25
8-9	24.97	18.88	24.77	16.39	12.98	2.02	0	0	0	0	9.20	3.11	-0.24
10-11	23.81	18.23	24.34	16.78	14.44	2.43	0	0	0	0	9.72	3.16	-0.28
14-15	23.38	17.9	23.68	16.58	15.28	3.14	0	0	0	0	10.07	3.22	-0.27
18-19	24.23	17.35	24.43	17.82	13.11	3.02	0	0	0	0	9.68	3.20	-0.28
22-24	23.34	17.71	25.2	18.15	14.28	1.34	0	0	0	0	9.66	3.10	-0.36
averages	*22.89*	*17.14*	*23.84*	*17.63*	*14.82*	*3.67*	*0.01*	*0*	*0*	*0.02*	*10.37*		
Core L-10													
0-0.5 (cm)	11.49	8.12	11.35	9.46	15.55	42.05	2.01	0	0	0	30.60	3.90	-0.94
1-1.5	19.2	14.56	20.59	16.89	17.66	10.31	0.77	0	0	0	13.71	3.56	-0.28
2-2.5	18.89	14.6	19.94	15.58	16.86	11.83	2.26	0	0	0	14.57	3.71	-0.21
4-4.5	21.92	16.63	21.63	14.57	12.12	9.93	3.2	0	0	0	12.43	3.79	-0.02
6-7	17.39	12.72	18.44	15.99	17.76	11.15	5.07	0.02	0	1.45	17.39	4.25	0.02
8-9	22.68	17.07	23.53	16.84	12.7	6.27	0.94	0	0	0	10.85	3.42	-0.13
10-11	22.27	16.11	21.86	15.11	11.53	7.43	5.68	0.01	0	0	12.44	3.96	0.04
14-15	24.52	18.61	24.79	16.48	11.01	4.34	0.28	0	0	0	9.57	3.23	-0.13
18-19	24.29	17.83	23.14	16.28	12.66	5.19	0.63	0	0	0	10.13	3.38	-0.12
22-23	22.32	17.06	24	18.25	13.85	4.32	0.16	0	0	0	10.53	3.24	-0.26
averages	*20.5*	*15.33*	*20.93*	*15.55*	*14.17*	*11.28*	*2.1*	*0*	*0*	*0.15*	*14.22*		
Core L-11													
0-0.5 (cm)	8.89	5.85	7.71	6.68	8.87	14.51	45.03	2.48	0	0	58.39	4.65	-1.11
1-1.5	9.56	6.22	8.56	7.05	7.55	13.5	45.63	1.94	0	0	55.11	4.83	-1.05
2-2.5	11.84	7.53	9.54	7.67	8.77	13.71	39.89	1.07	0	0	44.63	5.08	-0.82
3.5-4	10.66	6.67	8.92	7.07	7.48	13.22	44.04	1.92	0	0	51.17	5.04	-0.96
5-6	13.92	8.53	11.49	9.21	8.82	12.71	35.2	0.13	0	0	35.33	5.24	-0.64
7-8	13.42	9.01	11.64	8.82	8.8	12.3	35.23	0.78	0	0	36.45	5.27	-0.61
averages	*11.38*	*7.3*	*9.64*	*7.75*	*8.38*	*13.33*	*40.84*	*1.39*	*0*	*0*	*46.85*		
Surface samples HCl-treated													

TABLE I | **Continue.**

	GRAIN SIZE RESULTS (%)										TEXTURAL STATISTICAL PARAMETERS		
Sample	clay	VF silt	F silt	M silt	C silt	VF sand	F sand	M sand	C sand	>1 mm	Mean	S.D.	Skew-ness
L-A	8.36	5.25	6.05	4.05	2.86	0.58	2.1	11.59	18.29	40.9	160.40	8.74	-0.97
L-B	26.26	17.18	21.37	14.5	9.17	3.44	2.17	0	0	5.92	12.09	5.28	0.94
L-C	18.8	10.35	12.97	10.85	13.25	20.49	13.31	0	0	0	22.04	4.72	-0.33
L-D	7.96	4.87	5.92	4.04	2.82	2.9	12.89	30.79	26.64	1.17	147.70	6.72	-1.24
Surface samples HCl-untreated													
L-A	9.38	5.23	6.45	4.79	4.13	3.09	6.59	17.51	16.1	26.7	229.50	8.86	-1.19
L-B	13.38	7.98	10.11	7.13	5.46	3.08	5.12	14.49	19.77	13.4	83.20	10.00	-0.46
L-C	6.65	4.11	5.73	5.38	8.16	18.06	32.46	12.81	5.78	0.88	86.46	4.80	-1.13
L-D	2.46	1.51	1.93	1.44	1.36	1.68	7.66	19.34	21.95	40.7	454.60	4.08	-2.47
L-2	12.4	8.29	13.43	13.6	18.37	13.52	4.94	4.82	6.1	4.52	35.30	6.05	0.03
L-4	7.44	4.46	6.06	5.37	7.38	16.73	32.29	15.04	4.83	0.42	82.94	5.01	-1.13
L-5	18.01	11.75	17.74	16.01	17.4	11.33	3.55	0	0	4.21	18.49	4.98	0.24
L-6	12.55	8.56	13.51	12.78	17.13	18.01	13.34	2.05	1.49	0.65	29.97	4.80	-0.38
L-7	13.72	9.04	13.26	11.93	17.04	20.77	13.13	0.82	0.28	0	27.09	4.52	-0.55
L-8	22.72	16.07	22.8	17.25	17.48	3.67	0	0	0	0	10.72	3.35	-0.35
L-9	35.93	22.91	26.85	12.83	0.92	0	0	0	0	0.54	5.74	2.95	0.22
L-10	18.65	12.63	20.19	18.42	20.49	4.77	0	0	0	4.85	15.72	4.68	0.50
L-11	6.14	3.77	5.29	4.63	5.9	11.04	37.57	11.85	7.69	6.14	111.80	5.17	-1.12